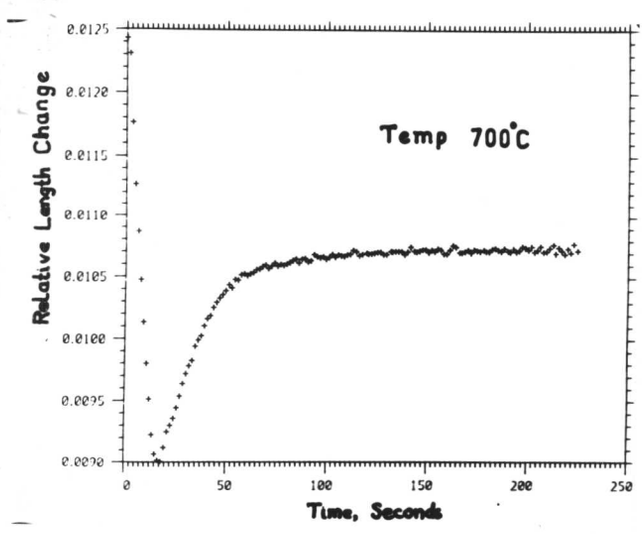

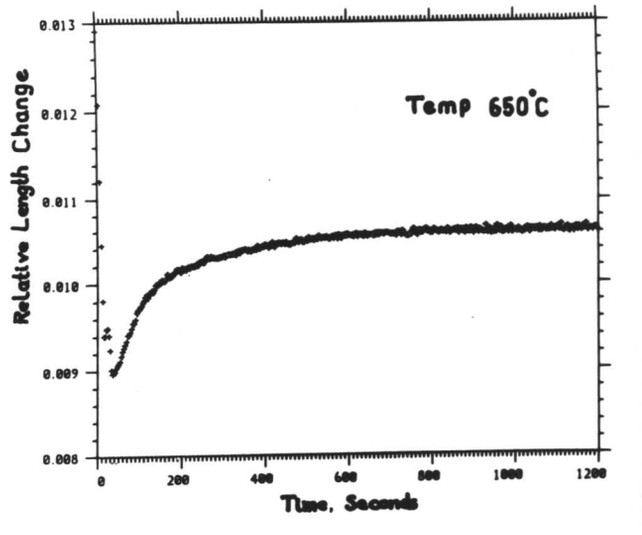

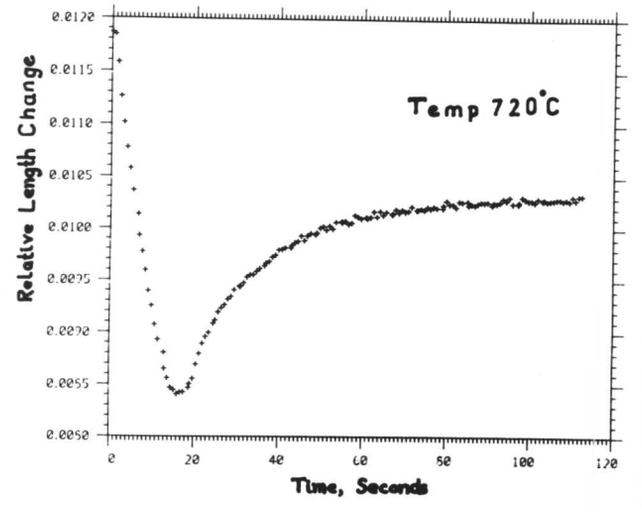

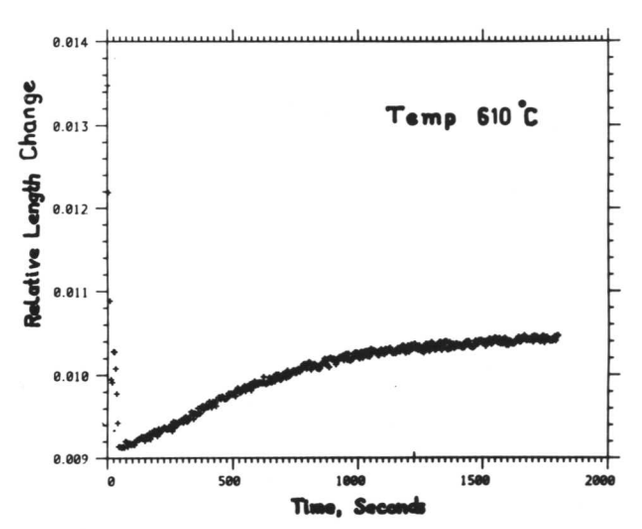

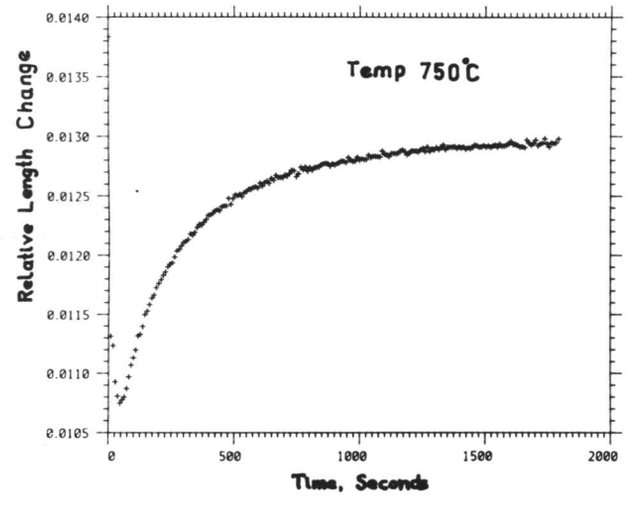

Figure 8.32: Plot of relative length change ($\frac{\Delta L}{L}$) vrs time at different isothermal temperature.

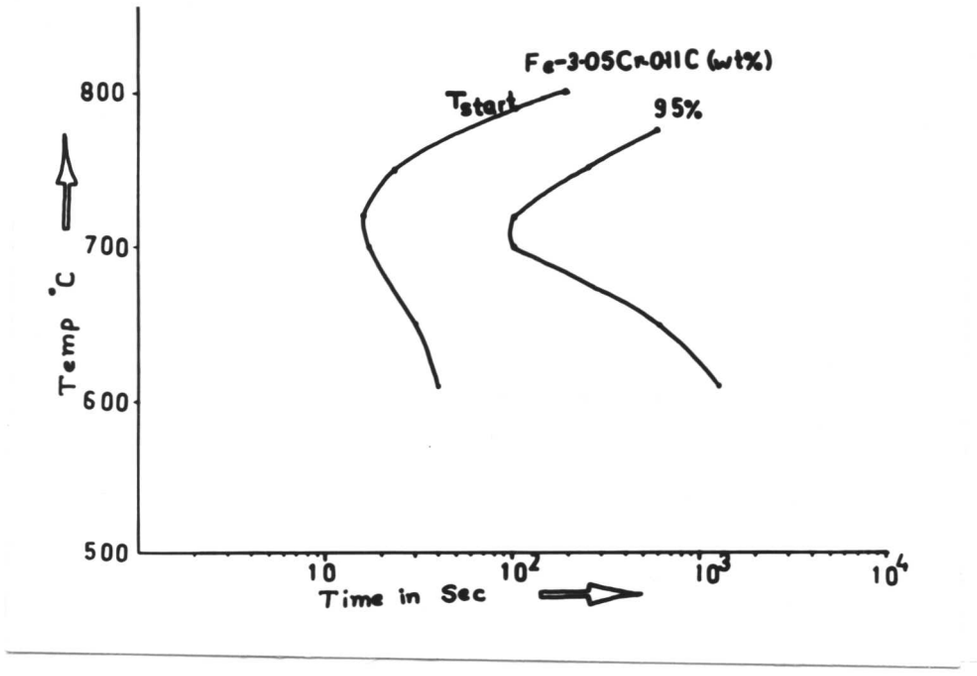

Figure 8.33: Experimentally determined TTT diagram.

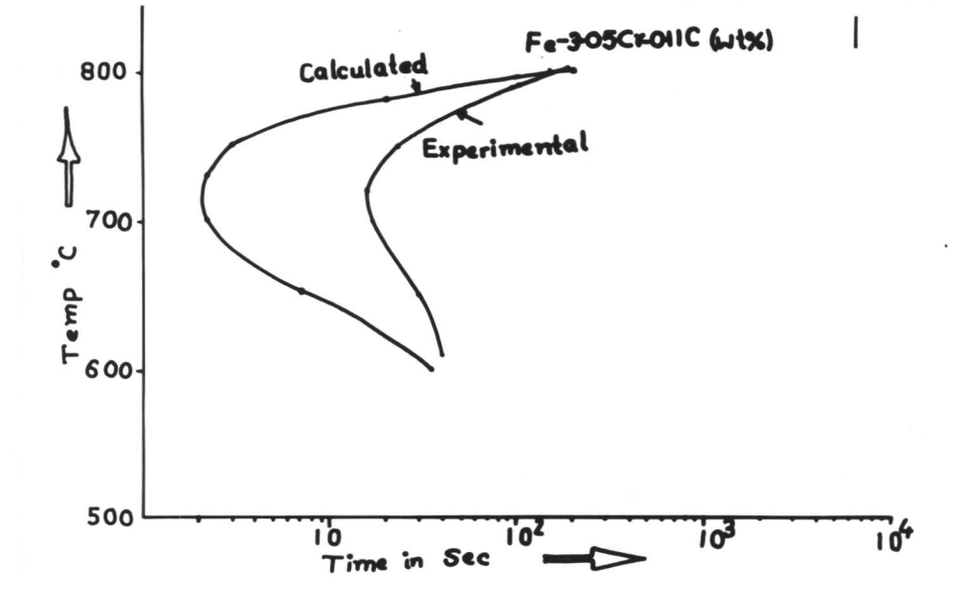

Figure 8.34: Showing comparison between calculated TTT and experimentally TTT diagram.

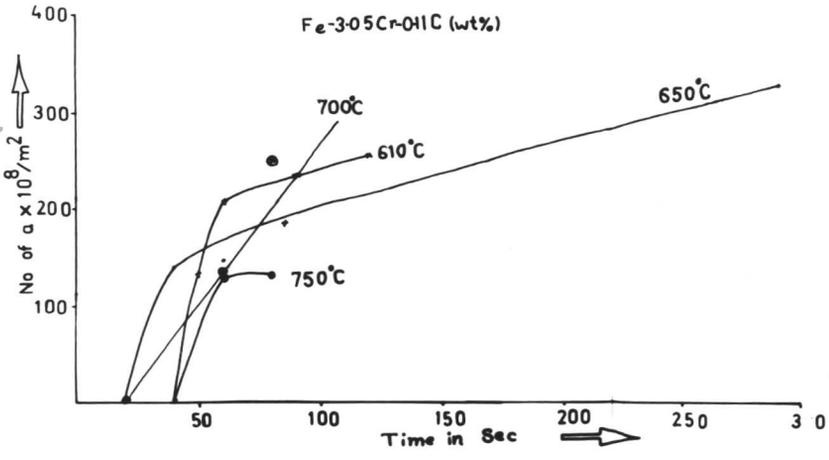

Figure 8.35: Plot of N_{α} vrs time.

CHAPTER IX

THE STUDY OF GROWTH KINETICS IN Fe-3.28Ni-0.11C (wt %) ALLOY

9.1 Introduction: This chapter is concerned with the growth kinetics of ferrite in a Fe-3.28Ni 0.11C(wt %) alloy. The choice of nickel as an alloying element appears to be ideal since it does not form any carbides. So the effect of carbide precipitation on the mobility of the γ/α interface can be minimized. It is thus expected that the $\gamma \rightarrow \alpha$ transformation will begin with the formation of virtually carbide-free proeutectoid ferrite. Parabolic growth rate constants determined from this allotriomorphic ferrite, as a function of isothermal transformation temperature, should provide a test for the various theoretical models (i.e. NPLE and PE) of diffusion-controlled growth.

9.2 Experimental Results: The exact composition of the alloy used was Fe-3.28Ni-0.11C (wt %). The details of the initial-heat-treatment given to this alloy have been already discussed in the Chapter II.

The alloy after austenitizing was subjected to isothermal transformation in the temperature range of 600°C to 700°C.

The TTT diagram for the beginning of austenite decomposition in this alloy was constructed on the basis of the model developed by Bhadeshia[1]. The calculated TTT curve for start of transformation is shown in Fig. 9.1a. This TTT curve was used to design the experiments and select the range of isothermal transformation.

Isothermal transformation at 700°C was carried out for different lengths of time. Optical microscopy showed that the observable nucleation of ferrite was recorded after 90 seconds at this temperature. (Fig. 9.2.) This incubation period is in close agreement with the one obtained from the calculated TTT curve which shows an incubation period of around 70 seconds. The nucleation of allotriomorphic ferrite occurred preferentially along prior austenite grain-boundaries. Growth followed rapidly along the grain-boundaries (i.e. lengthening). Its growth perpendicular to the grain-boundary occurred at a relatively low rate (i.e. thickening). With increasing time at the transformation temperature the ferrite grew rapidly along the grain boundaries to form a network (Fig. 9.3). These allotriomorphs of ferrite appeared to be "clean" with no evidence of interface pinning. The α/γ interface either appeared

planar or curved. No perturbations of the α/γ interface were observed. TEM observation could not detect any carbide precipitation during the early stages of transformation. However after prolonged transformation, extensive evidence of cementite was noticed. Two distinct modes of precipitation were observed. Fig. 9.4 shows precipitation of cementite on dislocations as well as in the matrix whereas Fig. 9.5 shows evidence of interphase precipitation. The plot of maximum half-thickness vrs square root of time is shown in Fig. 9.6. The slope of this curve for 700°C gives the value of parabolic rate constant as 0.43 $\mu m/\sqrt{sec}$. Fig. 9.6 also shows that the maximum half thickness of the ferrite is proportional to the square root of time indicating diffusion-controlled growth.

Isothermal transformation at 680°C led to the development of allotriomorphic ferrite at prior austenite grain-boundaries. The observable nucleation of ferrite was optically recorded after 30 seconds of incubation period. However the incubation period determined from the (Fig. 9.1) TTT curve is approximately 18-20 seconds which is slightly less than the optically recorded incubation period. The allotriomorphic ferrite formed a network along the prior austenite grain-boundaries with increasing isothermal time. (Fig. 9.7.) The parabolic growth rate constant was determined from Fig. 9.6 for 680°C as 1.02 $\mu m/\sqrt{sec}$. During the later stages of transformation precipitation of cementite on dislocations was observed using TEM. (Fig. 9.8.) A pearlitic structure was also observed in some areas as shown in Fig. 9.9. However, the allotriomorphic ferrite formed during the early stages of transformation (i.e. before 50 sec) remained free from cementite so that the measured parabolic growth rate constant should be reliable. Practically no evidence of interphase pinning was noticed. In some cases Widmanstätten ferrite was also observed. This is in close agreement with the theoretical calculation[17] which shows that Widmanstätten ferrite should begin to form in this range of 700°C - 660°C.

A slight increase in the parabolic growth rate constant to 1.2 $\mu m/\sqrt{sec}$ was observed at the isothermal temperature of 650°C (Fig. 9,6). Carbides were detected using TEM during the early stages of transformation at 650°C. These carbides, which are basically cementite, formed by three different mechanisms, Fig. 9.10 shows precipitation of cementite by the interphase mechanism. Occasionally precipitation on dislocations was also recorded as shown in Fig. 9.11. Formation of fibrous cementite appeared to be dominant at this temperature (i.e. 650°C Fig. 9.12) during the later stage of transformation. The calculated TTT curve shows an incubation period of 10 seconds whereas the optically determined value is 50 seconds. Transformation at 600°C followed the same general behaviour and the parabolic rate constant was found to be

1.2 μm/√sec. The data have been presented in Fig. 9.6. The observable (optically) nucleation of allortiomorphic ferrite started around 6 seconds, which is much faster than indicated in the calculated TTT curve.

The calculated TTT curve (for beginning of transformation) and the optically determined TTT curve (for observable nucleation of ferrite) were plotted in Fig. 9.1b. The TTT curves clearly show reasonable agreement at high temperatures (i.e. 700°C and 680°C) but they diverge at lower temperatures (i.e. 650°C and 600°C).

The calculated parabolic rate constants are plotted against temperature and compared with the experimentally determined values as shown in Fig. 9.13. There is good agreement in the temperature range 600°C to 680°C. But at a temperature of 700°C (close to the Ae_3 temperature), rather poor agreement is apparent.

Using the Quantimet 720, the volume fraction (V_α) was measured at successive intervals of time at each temperature and plotted against time. Figure 9.14 (a and b) shows a plot between V_α and time for temperatures, 600, 650, 680°C and 700°C. At least 10 fields were taken from each specimen to minimize the statistical error.

A curve was also plotted between log log $\frac{1}{1-V_\alpha}$ vrs log t, as shown in Fig. 9.15. From the slope of the this the value of n was determined. The values of 'n'are given (see Table 9.1).

9.3 Discussion

The experimental results indicate that the thickening of ferrite allotriomorphs occurs as a parabolic function of time (Fig. 9.6). This indicates that the interface moves under diffusion-control and does not seem to be limited by interface processes for the temperature range of 600°C to 700°C.[2]

The parabolic rate constants thus determined were plotted as a function of temperature and compared with the theoretically calculated values based on the paraequilibrium model (Fig. 9.13). Good agreement was observed in the temperature range 600°C to 680°C. Unlike Cr, nickel does not form any carbides, so that any "solute-drag-like" effect should be absent. This is consistent with experimental observations where not protuberances were detected on the γ/α interfaces. Secondly, nickel is believed to cause a high proportion of incoherent γ/α interface[3] thereby minimizing the effect of facetting on the mobility of γ/α interfaces. Except at 650°C, no carbide was detected during the early stages of transformation where most of the thickness measurements were done. Even at 650°C, not all the allotriomorphic ferrite exhibited cementite precipitation. This may be the reason why better agreement with calculated

parabolic rate constants is obtained for this alloy in the range of 700°C to 600°C. Fig. 9.15 shows a plot of log log $\frac{1}{1-V_\alpha}$ vrs log t. This was plotted to obtain the value of 'n' in Avrami's equation $V_\alpha = 1-\exp(-kt^n)$ where 'k' and 'n' are constants. Since the value of 'n' lies between 1.5 to 2.5, it was concluded that growth of allotriomorphic ferrite is consistent with diffusion controlled growth with decreasing nucleation rate.[4]

Microstructures: Carbide-free ferrite was detected at all temperatures (except at 650°C) during the early stage of transformation. The morphology of the ferrite obtained was consistent with Dubé's morphological classification.

Unlike the Cr-steel (where extensive evidence of interface pinning was noticed), this Fe-Ni-C alloy showed no evidence of serrated interfaces. All the interfaces were either planar or smoothly curved.

During the later stage of transformation four distinct modes of carbide precipitation were noticed:

1. Precipitation on dislocations, (Fig. 9.4).
2. Interface precipitation, (Fig. 9.5).
3. Fibrous precipitation, (Fig. 9.12.)
4. Pearlite , (Fig. 9.9).

1. Precipitation on dislocations: It has long been known that dislocations can act as sites for the nucleation of new phases. Cahn[5] has developed a model to estimate the effectiveness of a dislocation as a catalyst for such nucleation. In his model, he assumes that the nucleus of the precipitate lies along the dislocation core and is incoherent with the matrix. The lack of coherency between the two phases allows the relaxation of the stresses caused by the dislocation within the volume of the precipitation. This relaxation is the driving force for the precipitation on the dislocation. Formation of coherent precipitates on dislocations has also been reported[6]. In the present investigation, the carbides that formed on the dislocations were probably incoherent , since they did not give any strain-contrast[7].

2. Interphase-precipitation: In the absence of carbide forming elements like V, Ti, Cr, etc., it is possible for cementite to precipitate by an interphase-precipitation mechanism. Interphase-precipitation of cementite in Fe-C alloys has been previously reported[8, 9]. However in presence of carbide forming element, its precipitation at the advancing γ/α interface is replaced by alloy carbides. That is why in the case of steels containing carbide forming

elements, cementite is never reported to form at the advancing γ/α interface. The mechanism of interphase precipitation is discussed in the Chapter II.

3. Fibrous precipitation of cementite:- Fibrous precipitation of cementite in steel has never been reported earlier. Fibrous precipitation is similar to interphase precipitation in so far as it nucleates at the γ/α interface, but continues to grow in the direction of growth of the interface.

Whereas the interfaces for interphase-precipitation have a low interfaceal energy, the interfaces at which fibrous growth occurs are usually curved and of high energy. While the planar interfaces move by the ledge mechanism, the high energy curved interfaces move by unco-ordinated jumps of atoms across the interface. It is reported that the alloying elements which slow down the $\gamma \rightarrow \alpha$ transformation, increase the proportion of fibrous carbides. For example Mn & Ni addition lead to a higher volume fraction of fibrous type carbides.[10, 11] This result indirectly suggests that additions of Mn or Ni increase the proportion of incoherent interfaces which in turn favours the nucleation of fibrous carbides particularly at lower temperatures where the transformation is slowed down. This is consistent with the results obtained on isothermal transformation at 650°C.

Although in the present case, detailed crystallographic analysis has not been done due to lack of ability to retain the austenite at room temperature, the earlier workers[12, 13] have shown that the ferrite associated with fibrous carbide did not have a rational-orientation-relationship with adjacent austenite. But in the case of interphase precipitation the carbides are related to the ferrite either by K-S relationship[14] or Baker - Nutting relationships[15]. These carbides are also found to have a cube-cube relationship with the austenite.

4. Formation of pearlite: In addition to precipitation on dislocations, interphase and fibrous carbide precipitation, the formation of pearlite was also noticed. (Fig. 9.9). A full description of the mechanism of nucleation and growth of pearlite is beyond the scope of present investigation. However, it was generally noticed that the nucleation of pearlite nodules occurred at the prior austenite grain-boundaries. Pearlite is also found to nucleate on pro-eutectoid ferrite or cementite.

TTT Curve: Figure 9.1 shows the calculated TTT curve along with the experimentally (optically) determined TTT curve. Reasonable agreement was achieved at low undercoolings (i.e. at 700°C and 680°C) but at lower temperatures, (i.e. at 650°C & 600°C) the disagreement was significant. At

650°C, a bay in the TTT diagram was recorded, but the theoretically calculated TTT curve shows a bay at around 600°C. Such a bay in the TTT diagram is sometimes attributed to the solute-drag effect. However, the bay in the TTT diagram has been reported to occur due to two separate mechanisms.[1] The upper 'C' curve represents the diffusional transformation while the lower one represents the diffusionless transformation. Figure 9.1b also shows the TTT curve obtained by Shiflet et al.[16] Their TTT curve did not show any bay. Probably they might have missed the temperature at which the bay occurs. The reason for the lack of detailed agreement between experimental and calculated values can be understood on the basis of microstructural evidence. The ferrite which formed at higher temperatures was free of cementite, but not always at lower temperatures.

The calculations used for constructing TTT curves do not allow for effect of carbide formation on driving force. This may be the reason for discrepancies in the results where carbide precipitation was observed. The details of TTT calculation are discussed in the Appendix 1.

9.4 Conclusions

1. Good agreement was achieved between the experimentally determined parabolic growth-rate constants and theoretically calculated values based on the paraequilibrium model for diffusion-controlled growth for the temperature range of 700°C to 600°C (Fig. 9.13).

2. The $\gamma \rightarrow \alpha$ transformation always started at austenite grain-boundaries. The heterogeneous nucleation of the allotriomorphic ferrite at these boundaries is preferred because the nucleation of α at these heterogeneous sites results in significant decrease in the activation energy barrier required for nucleation. It also leads to an overall decrease in the surface energy by eliminating part of the grain boundary surface area.

3. Except at 650°C, the $\gamma \rightarrow \alpha$ transformation started with the formation of clean ferrite. However, during the later stages of transformation four distinct modes of carbide precipitation were noticed. These include precipitation on dislocations, interphase-precipitation, fibrous carbide precipitation and pearlite.

4. The theoretically calculated TTT curves matched well with the experimentally experimentally determined TTT curve at low undercoolings (i.e. at 700°C and 680°C). However, at lower temperatures (i.e. 650°C and 600°C) the agreement was poor. The reasons for disagreement have been discussed on the basis of available microstructural observations. It is believed that the formation of carbide

along with the ferrite alters the thermodynamic conditions and hence affects the result adversely.

TABLE 9.1

$$V\alpha = 1-e^{-kt^n}$$

Temp °C	n
600°C	1.66
650°C	2.00
680°C	2.12
700°C	2.4

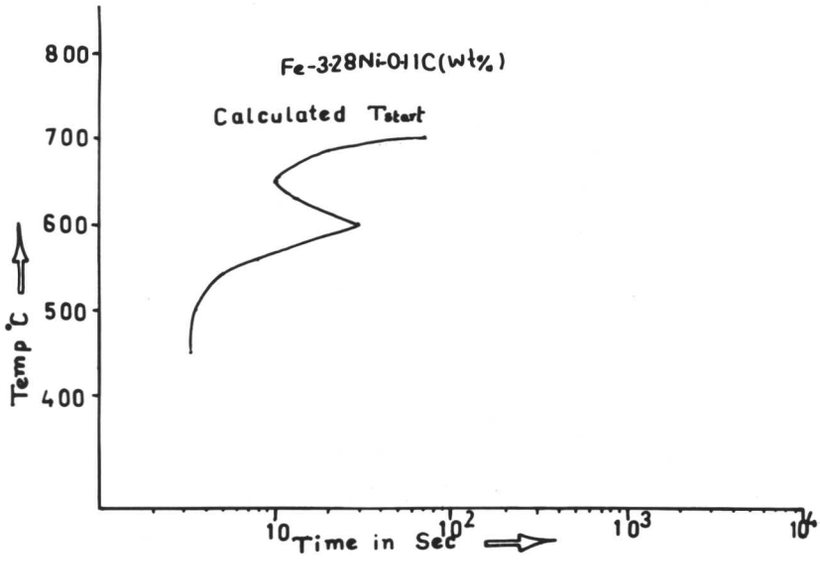

Figure 9.1a: Calculated TTT curve for start of transformation in Fe-3.28Ni-0.11C (wt%) alloy.

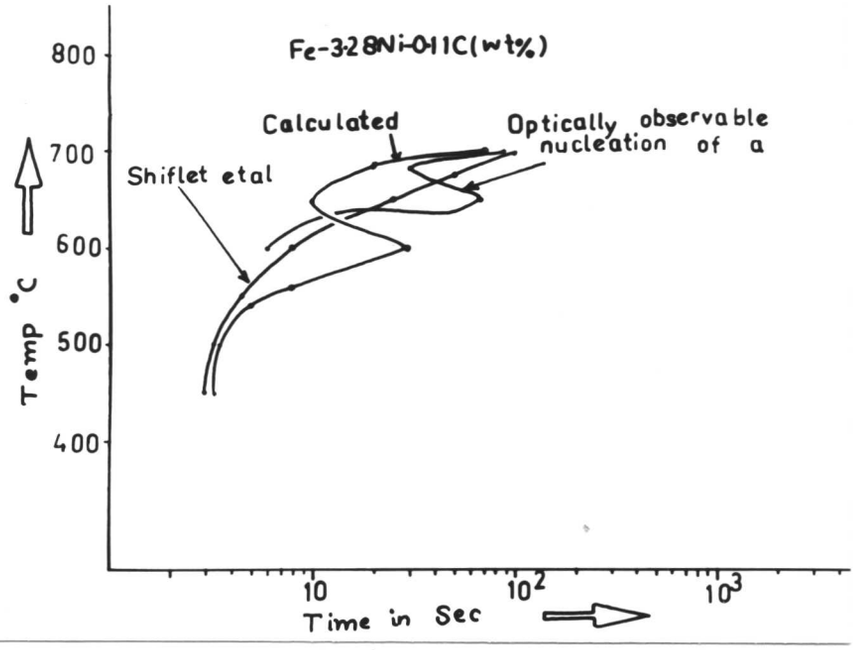

Figure 9.1b: Calculated TTT curve compared with experimentally determined TTT curve.

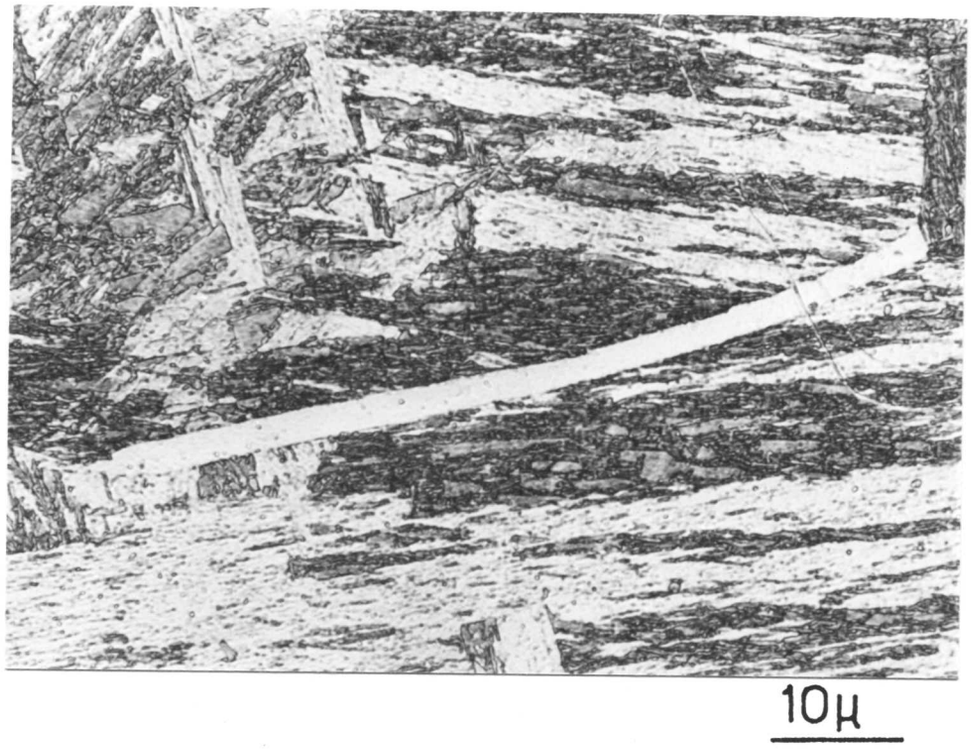

Figure 9.2: Grain-boundary allotriomorphic ferrite showing high aspect ratio. It is also virtually free of carbides (700°C/90 sec).

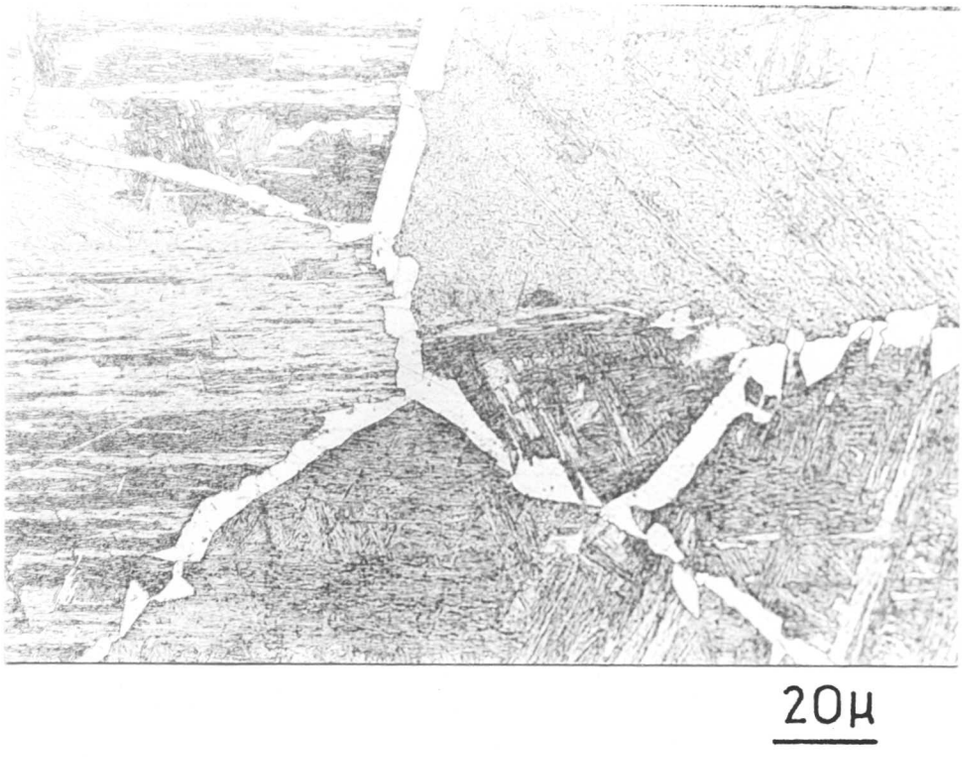

Figure 9.3: Network of allotriomorphic ferrite along the prior austenite grain-boundaries. (700°C/4 min).

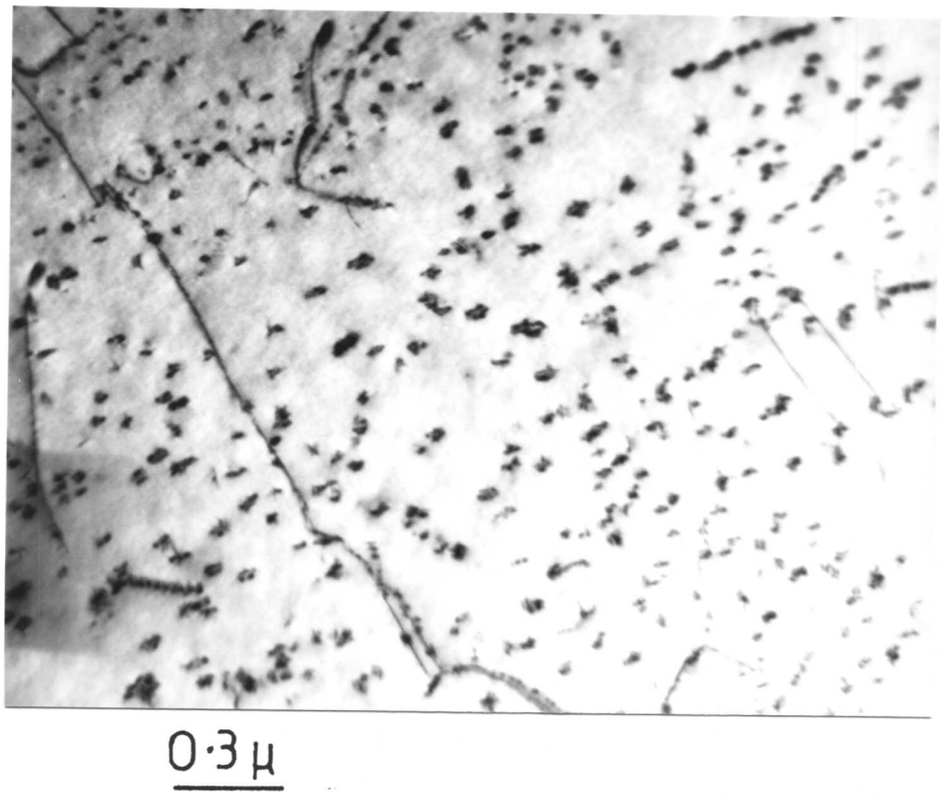

Figure 9.4: Precipitation of cementite on dislocations. (700°C/2 hrs).

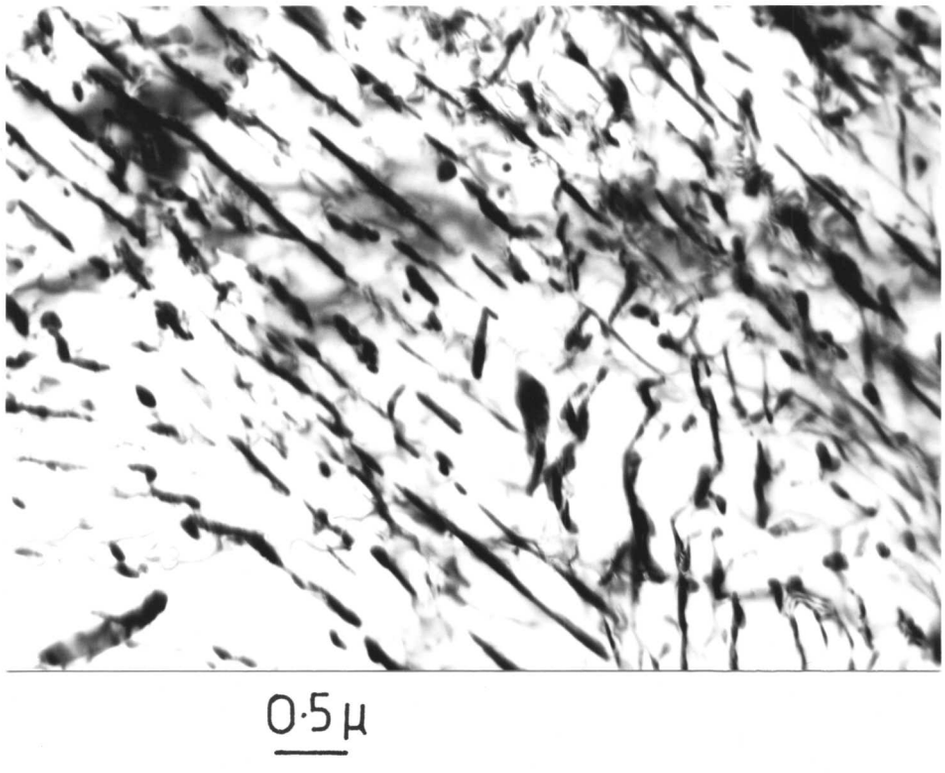

Figure 9.5: Cementite possibly formed by interphase-mechanism. (700°C/2 hrs).

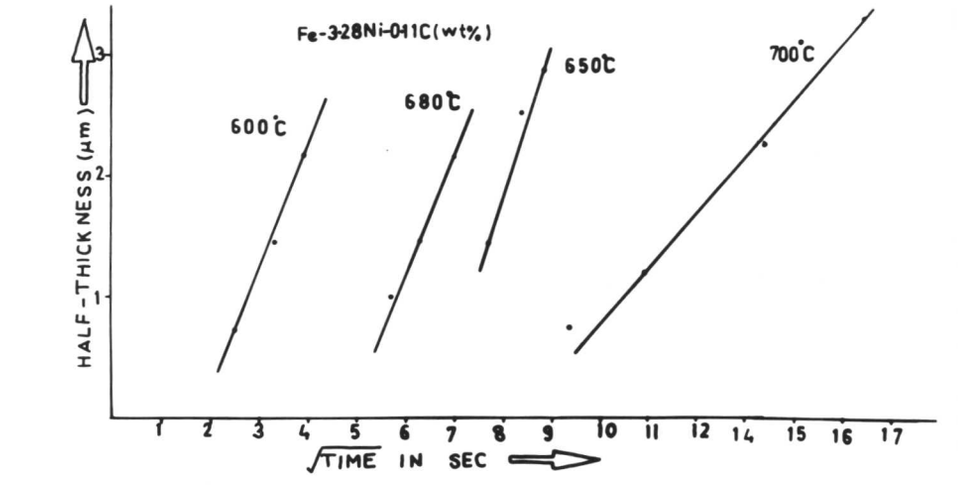

Figure 9.6: Plot of half thickness of ferrite vrs square root of time.

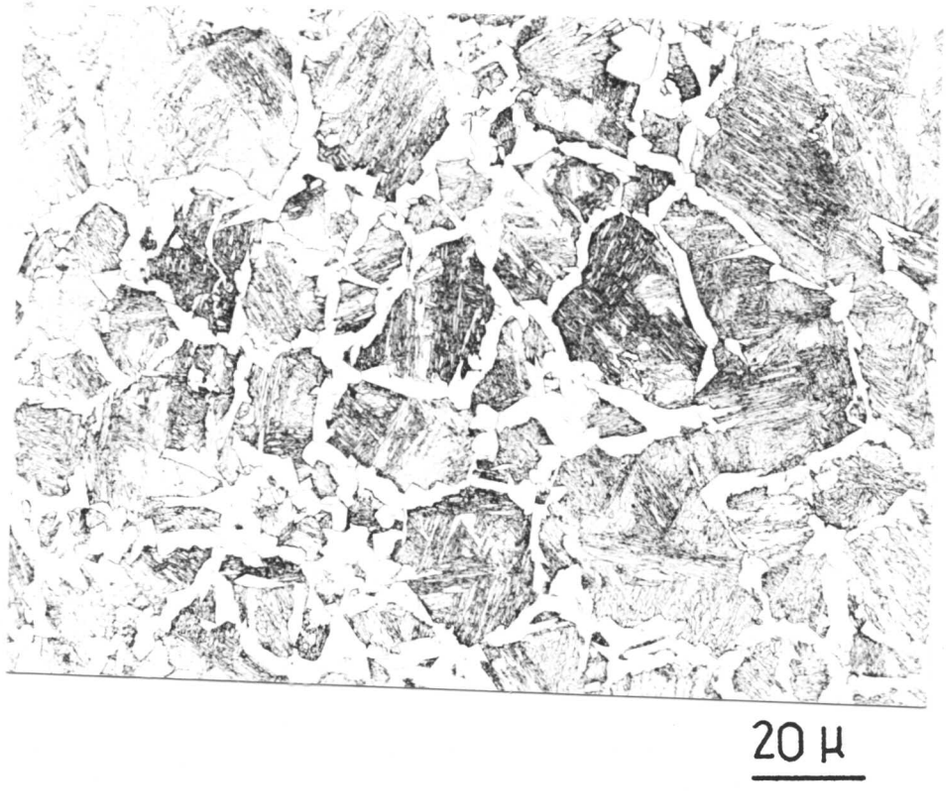

Figure 9.7: Net-work of allotriomorphic ferrite along prior austenite grain-boundaries (680°C/50 sec).

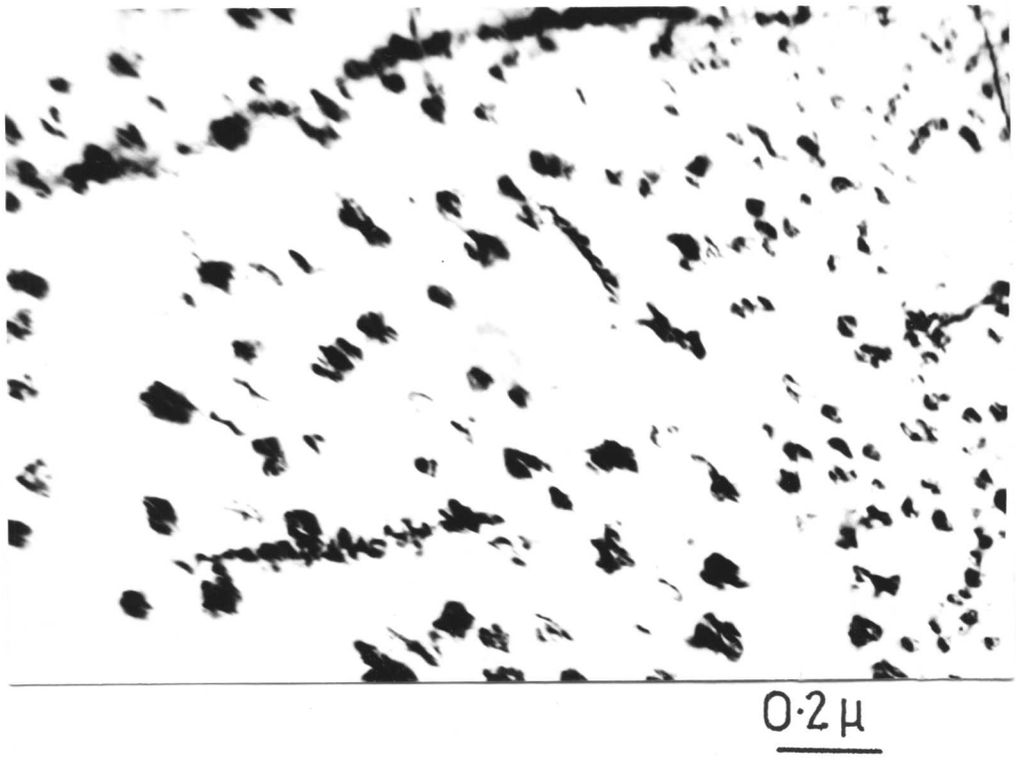

Figure 9.8: Precipitation of cementite on dislocations within the ferrite.

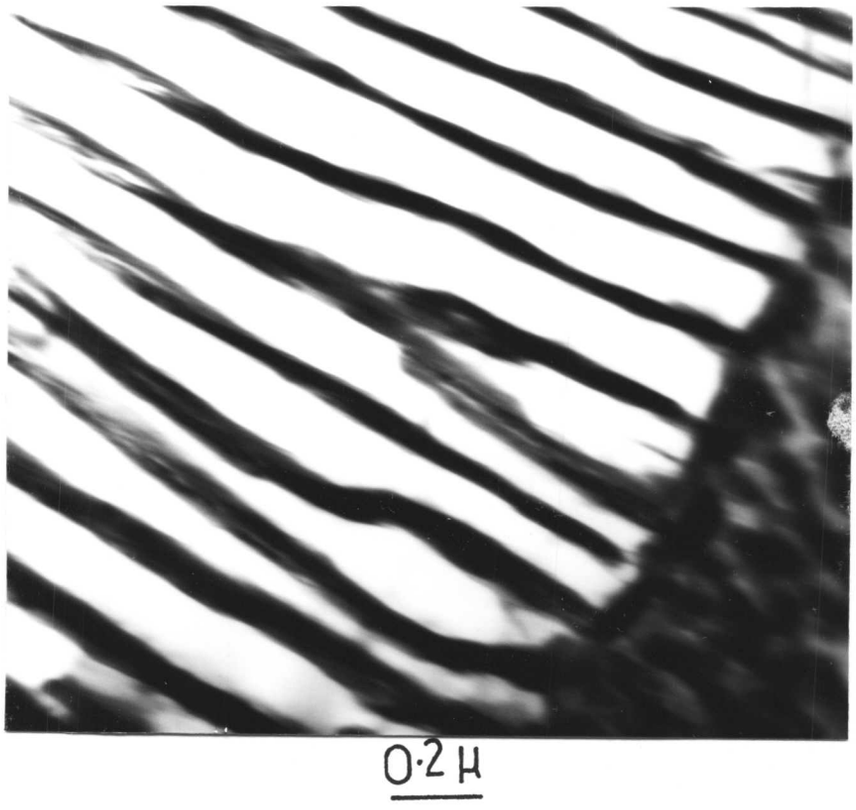

Figure 9.9: Pearlitic structure

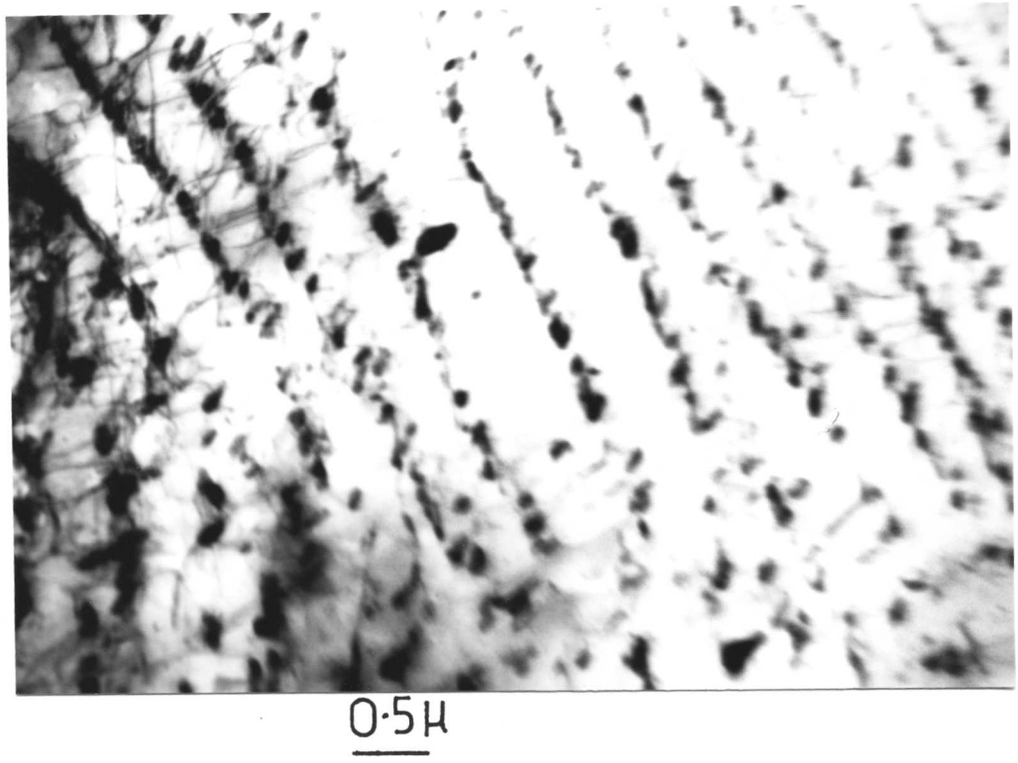

Figure 9.10: Precipitation of cementite by interphase mechanism.

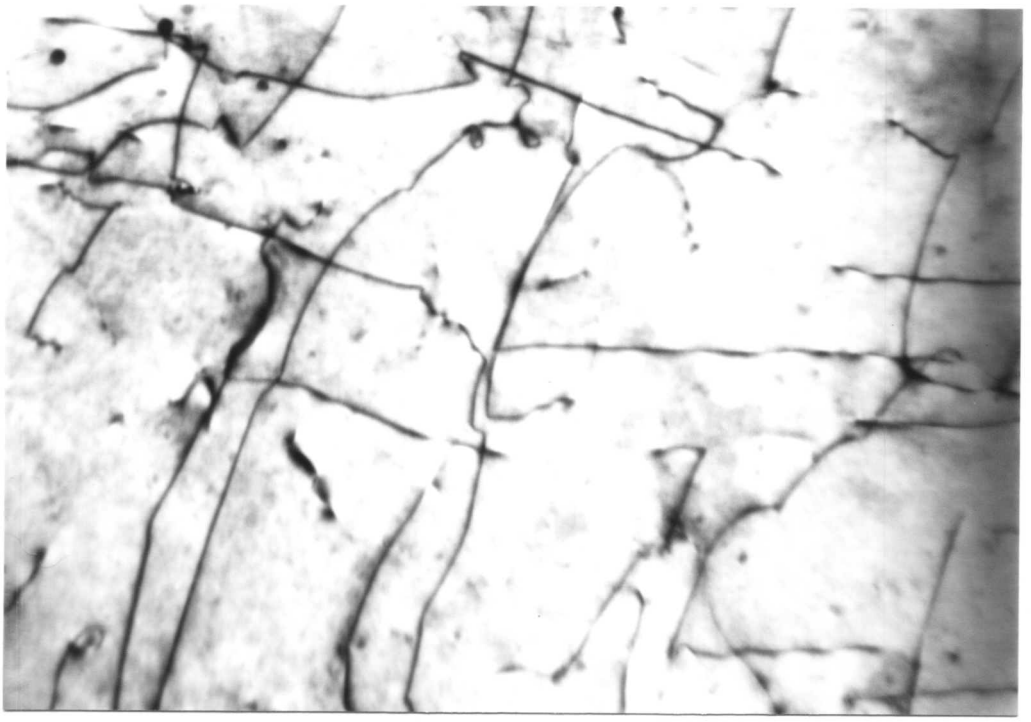

Figure 9.11: Precipitation of cementite on dislocations.

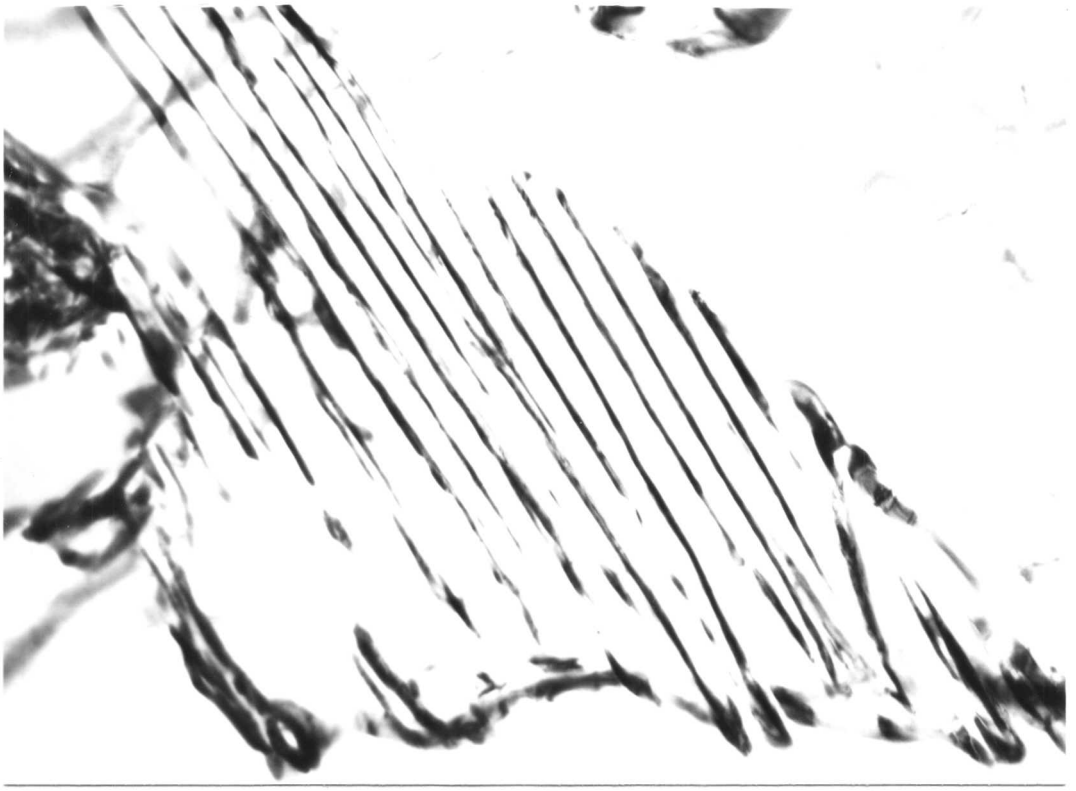

Figure 9.12: Precipititation of cementite in fibrous mode. 0·5 μ

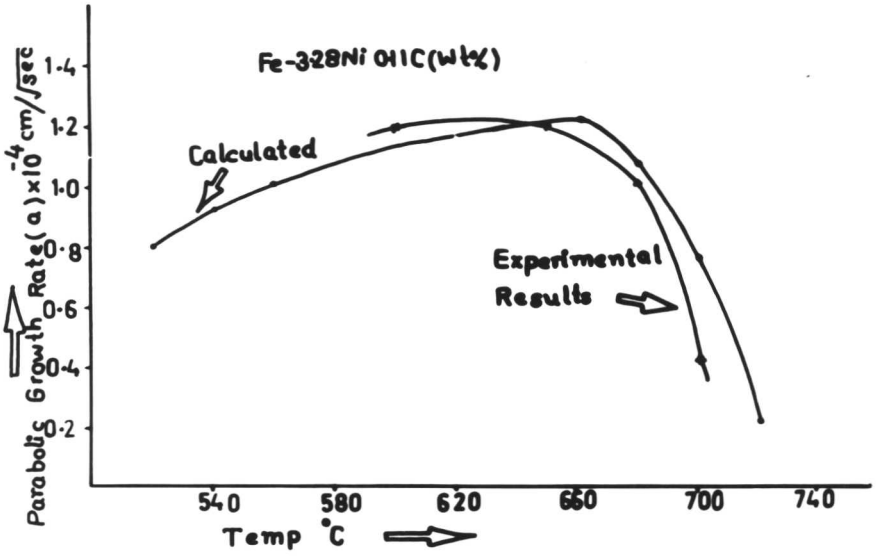

Figure 9.13: Plot of parabolic growth rate constant vrs temperature.

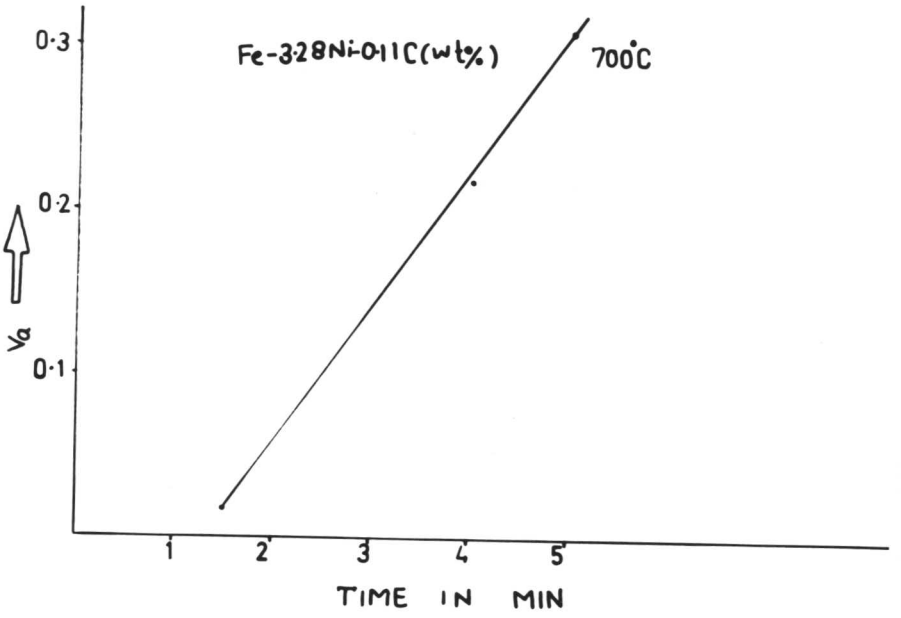

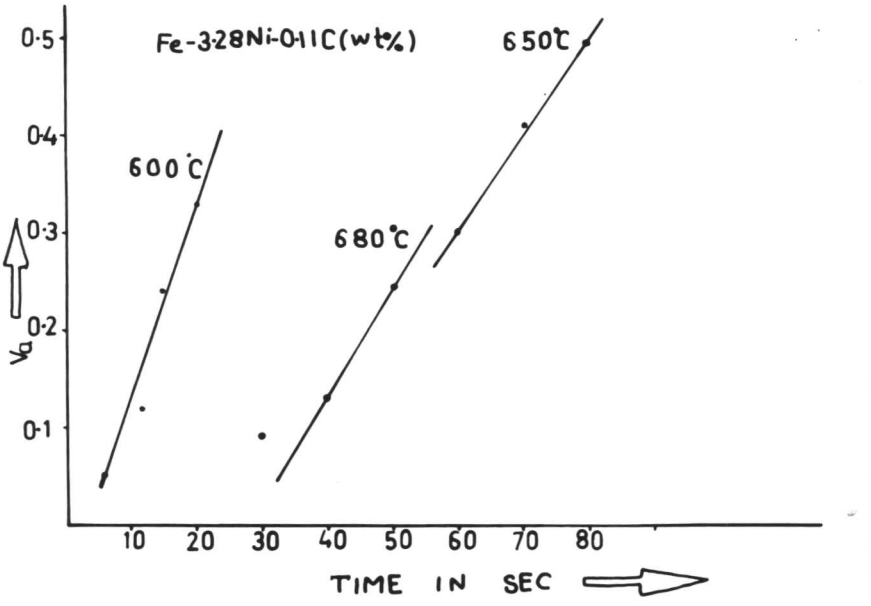

Figure 9.14a and b: Volume fraction of ferrite against time is plotted.

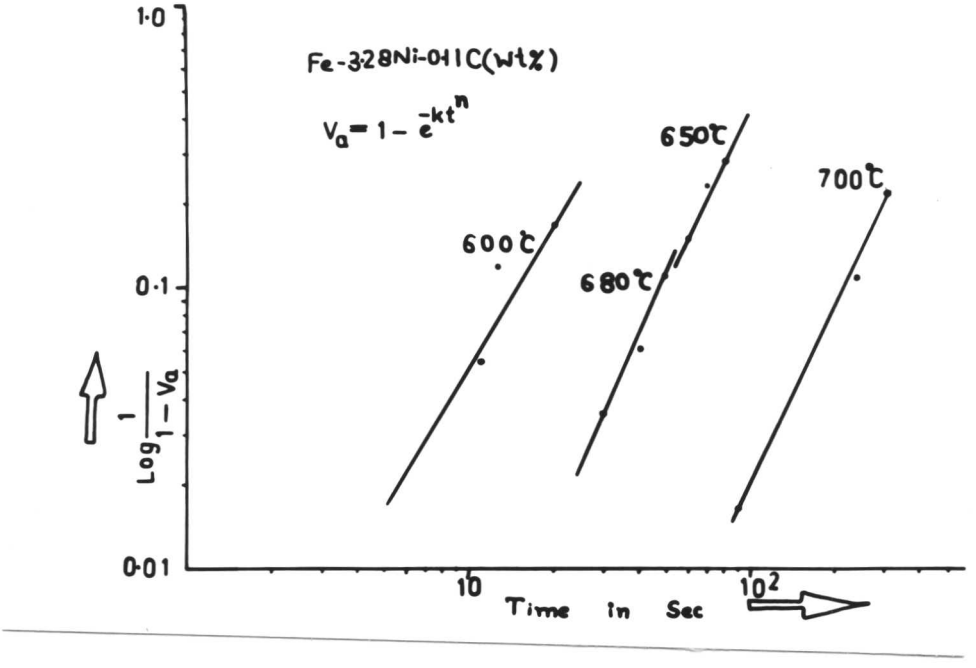

Figure 9.15: Plot of log log $\frac{1}{1-V\alpha}$ vrs log t, this is also known as Avrami's plot.

CHAPTER X

CONCLUSIONS AND SUGGESTIONS FOR FUTURE WORK:

10.1 Conclusions:

1. Silicon has a pronounced effect on enhancing interphase precipitation at high transformation temperatures. It expands the α-phase field and lowers the solid solubility of the carbides in ferrite. In addition, it has a strong tendency towards developing a high proportion of γ/α semi-coherent interfaces which move by a ledge mechanism. It can be anticipated that these factors may combine to enhance interphase precipitation in Fe-5.5W-2.03Si-0.37C (wt%) alloy. Silicon also accelerates the kinetics of the $\gamma \rightarrow \alpha$ transformation.

2. Interphase precipitation is not only limited to the less mobile semi-coherent γ/α interfaces but it can also occur on more mobile ledges. This directly contradicts the hypothesis proposed by Honeycombe. According to his hypothesis, the high mobility of the ledges provides least opportunity for nucleation to occur there. Consequently nucleation takes place on less mobile semi-coherent interfaces.

3. Ledges may vary in height even at the same temperature and this variation may be an order of magnitude. The variation in ledge height occurs as a result of ledge multiplication during the transformation. However, some workers have reported that the ledge height depends upon the temperature and alloy composition. And it increases with increasing temperature.

4. Frequent evidence of cusps on semi-coherent low energy interfaces was noticed at the highest transformation temperatures. These cusps are developed as these interfaces move across the carbides during the transformation. Presence of cusps on low energy facets led to the view that these interfaces have moved normal to it in a way similar to that of incoherent interfaces. This contradicts the classical view the magnitude of the critical driving force required to move low energy facets is so high that it is never achieved in practice.

5. The alloy with the same chemical composition but without silicon showed a tendency to contract the α-phase field. Random dispersion of tungsten carbide was frequently observed in this alloy. The volume fraction of these carbides was found to increase with decreasing temperature. These carbides has formed from super-saturated ferrite or interphase precipitation at the incoherent γ/α interface.

6. Pinning of the incoherent as well as semi-coherent interface was recorded at all temperatures of transformation in Fe-5.8W-0.4C (wt%) alloy. The morphology of the γ/α interface appeared serrated as well as ragged. Serrated interface indicates that the pinning has occurred due to interphase carbide precipitation at the incoherent γ/α interface. Protuberances on the interface developed as the γ/α moved across the carbide particles present in the austenite. Interphase precipitation was less pronounced in this alloy.

7. When the carbon content is reduced from 0.4 to 0.23C wt% keeping the tungsten content the same, the α-phase field is expanded (Chapter V). The kinetics of the $\gamma \rightarrow \alpha$ transformation are accelerated by reducing the carbon level of the alloy. The ferrite formed during the early stage of transformation was found to be virtually free from carbides. No evidence of interphase precipitation was noticed in this alloy during the early stage of transformation. However, during the later stage of transformation at 850°C, the carbide precipitation started at the α/γ interface but appeared to grow in austenite. The sequence of the reaction that occurred at 850°C can be represented by

$$\gamma \rightarrow \alpha + \gamma_1 \rightarrow \alpha + M_6C + \gamma_2 \rightarrow \alpha + M_6C$$

A small addition of titanium (0.14 wt%) (i.e. Fe5.9W-0.14Ti-0.21C (wt%)) showed a dramatic effect on suppressing the kinetics of transformation in Fe-W-C alloys in the temperature range of 700°C-900°C.

8. The transformation characteristics of Fe-5W-2.3Si-0.15C wt% alloy is compared with that of Fe-5W-0.23C wt% alloy (Chapter V and VI). The alloy containing silicon again shows the tendency towards accelerating the interphase precipitation at the highest transformation temperature (850°C). But at lower transformation temperature (700°C), fine dispersion of alloy carbides is noticed within the α-ferrite. These fine dispersions of alloy carbides are formed from supersaturated ferrite and not by interphase mechanism. These carbides are surrounded by a PFZ within the ferrite grain.

It is also noticed that a grey rim appeared at the γ/α interface but grew in the austenite. With increasing time, the grey rim grew in size to consume the whole austenite grain. Occasionally a dark etched region appeared ahead of the growing rim. Optically no information could be obtained concerning the microstructural constituents of the growing grey area. But transmission electron microscopy revealed that it contains fine particles of carbides along with some coarse carbides. Microstructural features of this rim are similar to those observed in many discontinuous reactions. It is interesting to note that the reaction has occurred during the later stages of transformation. No such observations are recorded in the case of alloys containing no silicon. The rate of transformation at all temperatures (850°C - 700°C) is enhanced by the addition of silicon. The α-phase field is expanded and the solubility of carbides in the α-ferrite is greatly reduced by the addition of silicon. A high proportion of facetted low energy interface is also noticed at all transformation temperatures.

8. Rare evidence of Widmanstätten ferrite was noticed for transformations in the temperature range of 850°C - 700°C. During the early stages of transformation, ledges appeared frequently in all the alloys, but this frequency of ledges appeared more in alloys containing silicon.

9. The $\gamma \rightarrow \alpha$ transformation started at the austenite grain-boundary and grew along it to form allotriomorphs. The aspect ratio of these allotriomorphs increased with decreasing transformation temperature. These phenomena were observed in all the alloys investigated.

10. Formation of tungsten carbide (WC/M_6C) along the prior austenite grain-boundaries by pre-precipitation led to drastic drop in nucleation rate at low undercoolings (i.e. 800°C). Pre-precipitation induces the formation of copious precipitates of tungsten carbides along the austenite grain-boundaries. Presence of these carbides on active nucleation site are held responsible for dramatic drop in nucleation rate of α (Fig. 7.4 Chapter V).

11. The growth kinetics were studied in Fe-C-X alloys (Chapter VIII & Chapter IX). The nickel steel (i.e. Fe-3.28Ni-0.11C (wt%)) showed a good agreement between the experimentally determined growth rate and theoretically calculated value based on para-equilibrium model for diffusion controlled growth in the temperature range of 700°C to 600°C (Fig. 9.13). But in case of chromium steel, the agreement was rather poor. The discrepancies in our results have been attributed to the presence of facetting, solute-drag-like

effect, pinning of the γ/α interface by carbide; interaction of clusters with interfaces and stereological error.

10.2 Suggestions for Further Work

1. It is essential to examine the precise role played by silicon during the transformations at various transformation temperatures in Fe-C-X alloys.

2. A theoretical analysis concerning the effect of silicon on solid-solubility product will be helpful in understanding the complex nature of carbide precipitation.

3. To develop a model to calculate the critical driving force required to move the semi-coherent interface as a function of alloy composition.

4. Mechanisms of ledge nucleation as a function of temperature and alloy composition are needed to understand the mobility of the semi-coherent γ/α interface.

5. A model like Orowan bowing mechanism, is required to study the effects of pinning on the mobility of the γ/α interface. Such a model will be helpful in understanding the growth kinetics in steels contianing carbide forming elements like (Ti, Cr, Nb, W, Mo, etc).

6. To develop an expression to calculate the activation energy of nucleation at the γ/γ grain-boundary and at the carbide/austenite boundary as a function of temperature.

7. High resolution microanalysis in Fe-C-X alloys is need to establish the exact mode of growth (i.e. PE or NPLE) over a range of isothermal temperature.

8. It is essential to study the effect of alloying element on the morphology of the allotriomorphic ferrite as a function of temperature.

APPENDIX I

CALCULATIONS USED FOR CONSTRUCTING TTT DIAGRAMS:

Bhadeshia[1] developed a thermodynamic model to predict the isothermal transformation diagrams simply from a knowledge of the chemical composition of the steel. This model utilizes Russell's theory[2, 3] for calculating the incubation periods normally associated with TTT diagrams (i.e. the time period before the onset of a detectable amount of isothermal transformation, t_s). The incubation period (t_s), for nucleation at grain boundaries can be expressed[2, 3] as

$$t_s = \frac{T}{(\Delta F_m^v)^p D} \qquad \text{(A.1.1)}$$

where T = Absolute temperature.

D = An effective diffusion coefficient related to boundary or volume diffusion, depending on the coherency state of the nucleus concerned.

ΔF_m^v = the maximum volume free energy change accompanying the formation of a nucleus in a large amount of matrix phase.

p = An exponent whose magnitude is a function of the nature of the nucleus. Russell obtained p = 2 for coherent nucleus and p = 3 for an incoherent one.

The effective diffusion coefficient (D) is expressed in terms of entropy (s) and enthalpy (Q) for diffusion[4] as follows:

$$D \propto \exp(S/R) \exp(-Q/RT) \qquad \text{(A.1.2)}$$

Substituting this value of D in equation A.1.1, and multiplying ΔFm^v by the molar volume of ferrite, we get

$$\text{In} \left[(\Delta F_m^v)^p \, t_s/T \right] = Q/(RT) + C_1 \qquad \text{(A.1.3)}$$

where C_1 is a constant.

The numerical value of the chemical free energy change (ΔFm) accompanying the formation of 1 mole of nucleating phase in a large amount of matrix phase can be estimated as follows using the principle of parallel tangent construction[5] (Fig. A.1.1)

$$\Delta F_{Fe}^{\gamma \rightarrow \alpha} + RT \ln \frac{a_{Fe}^{\alpha}(1-C)}{a_{Fe}^{\gamma}(1-\bar{C})} - RT \ln \frac{a_{C}^{\alpha}(C)}{a_{C}^{\gamma}(\bar{C})} = 0 \quad \ldots\ldots\ldots\ldots\ldots \quad (A.1.4)$$

$$\Delta F_{m} = RT \ln \left[\frac{a_{C}^{\alpha}(C_{m})}{a_{C}^{\gamma}(\bar{C})} \right] \quad \ldots\ldots\ldots\ldots\ldots\ldots\ldots\ldots\ldots \quad (A.1.5)$$

where $a_{Fe}^{\alpha}(1-C)$ refers to the activity of iron in ferrite evaluated at the concentration $(1-C)$ and a similar rationale applies to the other activity terms. The term $\Delta F_{Fe}^{\gamma \rightarrow \alpha}$ refers to the free energy change accompanying the austenite - ferrite transformation in pure iron and R is the gas constant. The term $\bar{C}$ is the average carbon concentration of the steel concerned and C_m represents the composition of ferrite which satisfies equation (A.1.4).

The ideal nucleus composition is obtained by iteratively solving equation (A.1.4). The value of ΔF_{m}^{v} is obtained by substituting the nucleus composition in equation (A.1.5).

For alloy steels, the first term of the equation (A.1.4) is replaced by

$$\Delta F_{Fe}^{\gamma \rightarrow \alpha} \left\{ T - 100 \sum_{i} Y_i \Delta T_{magi} \right\} + 141 \sum_{i} Y_i (\Delta T_{magi} - \Delta T_{nmi})$$

where the terms in the curly brackets are to be interpreted as the arguments of the function $\Delta F_{Fe}^{\gamma \rightarrow \alpha}$. Y_i is the mole fraction of the ith substitutional alloying element and ΔT_{magi} and ΔT_{nmi} are the displacements in the temperature at which the free energy change accompanying the austenite - ferrite in pure iron is calculated, in order to account for the changes in the magnetic and non-magnetic components of $\Delta F_{Fe}^{\gamma \rightarrow \alpha}$ respectively.

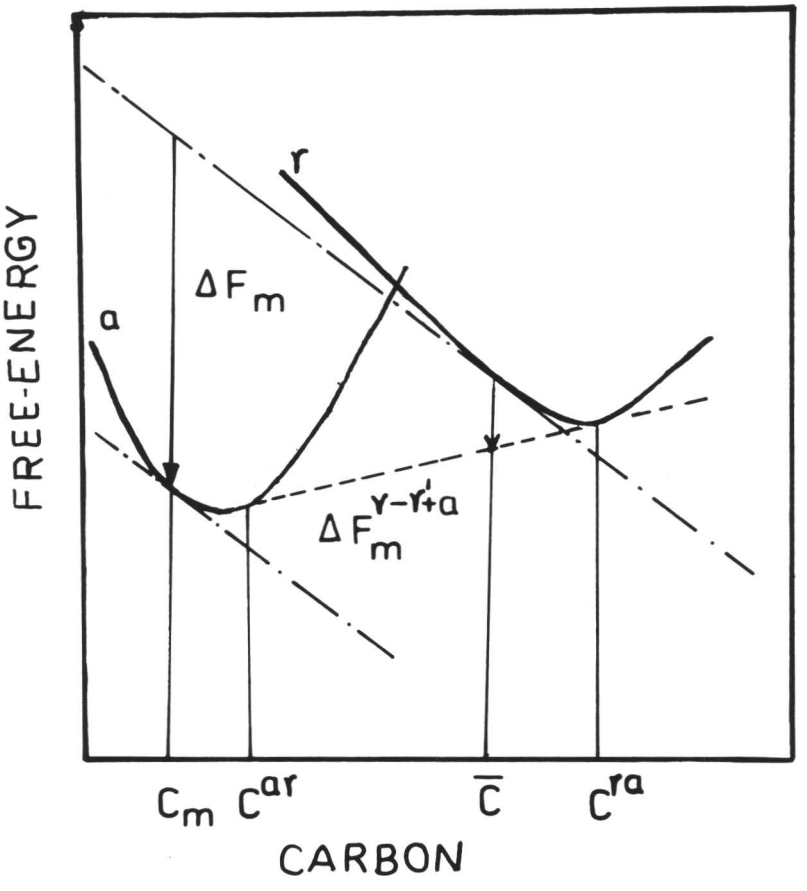

Figure A1.1: Schematic diagram showing free energy change during the $\alpha \rightarrow \gamma$ transformation.

APPENDIX II

A REVIEW ON THERMODYNAMICS OF DIFFUSIONAL DECOMPOSITION OF AUSTENITE:

In the present section, it has been tried to review in brief the thermodynamic analysis of diffusional decomposition of austenite. Such analysis are often vital importance to the metallurgist. Not only it provides with a better understanding of the factors influencing the transformation characteristics but also leads to precise assessment of the data needed in such studies. Within the past decade noteworthy progress has been achieved in developing more refined thermodynamic analysis.

Zener[1] using the thermodynamics of interstitial solid solution developed relationships for thermodynamic quantities of interest in the austenite → ferrite transformation. He assumed an ideal value of the positional entropy of carbon in austenite as well as ferrite. Although this method is less accurate than those developed later on, it turns out to be the only one presently feasible for a study of the influence of alloying elements upon the thermodynamics of the proeutectoid ferrite reaction. Subsequently Zener[2] realised the contribution of magnetic and non-magnetic component of pure iron towards change in free energy during $\gamma \rightarrow \alpha$ transformation. He also assumed that these components are affected by the alloying elements separately. For pure iron, the change in chemical free energy can be expressed as

$$\Delta F_{Fe}^{\gamma\rightarrow\alpha} = \Delta F_{FeNM}^{\gamma\rightarrow\alpha} + \Delta F_{FeMag}^{\gamma\rightarrow\alpha} \quad .. \quad .. \quad .. \quad .. \quad .. \quad .. \quad .. \quad .. \quad .. \quad \text{(A2.1)}$$

where $\Delta F_{FeNM}^{\gamma\rightarrow\alpha}$ and $\Delta F_{FeMag}^{\gamma\rightarrow\alpha}$ are the non-magnetic and magnetic components respectively of this free energy change. The non-magnetic component is free-dominant at temperatures below 600°C where $\Delta F_{FeMag}^{\gamma\rightarrow\alpha}$ is assumed to be negligible.

For Fe-X alloys, the equation developed[3] may be written as

$$\Delta F_{FeNM}^{\gamma\rightarrow\alpha} = 1.41\ (T - Y.\Delta_{NM}^{T} - 1013) \quad .. \quad .. \quad .. \quad .. \quad .. \quad .. \quad .. \quad .. \quad \text{(A2.2)}$$

where Y = atom per cent of X in either phase

ΔT = displacement in the temperature per atom per cent

The total free energy change for transformation of austenite to ferrite of the same composition in Fe-X alloys at temperature T is written as

$$\Delta F^{\gamma\to\alpha}{}^{1} = \Delta F^{\gamma\to\alpha}_{FeNM}\left[\ T-Y.\Delta T_{NM}\ \right] + \Delta F^{\gamma\to\alpha}_{FeMag}\left[\ T-Y.\Delta T_{Mag}\right] \quad .. \quad .. \quad .. \quad .. \quad (A2.3)$$

$\Delta T_{Mag} > \Delta T_{NM}$ for austenite stablizing elements and $\Delta T_{Mag} < \Delta T_{NM}$ for ferrite stablizing elements. For Fe-C-X alloys the total change in free energy without partioning of alloying elements or carbon may be written[3] as

$$\Delta F^{\gamma\to\alpha}{}^{1} = (1 - x_\gamma)\ \Big[\ 141y_\gamma\ (\Delta T_{Mag} - \Delta T_{NM}) + \Delta F^{\gamma\to\alpha}_{Fe}\ \Big(\ T - 100y_\gamma\ \Delta T_{Mag}\Big) +$$

$$x_\gamma\ (K-RT\ \ln\ 3)\Big] \quad .. \quad .. \quad .. \quad .. \quad .. \quad .. \quad .. \quad .. \quad .. \quad .. \quad .. \quad (A2.4)$$

where K = Free energy to transfer 1 mole of carbon from asutenite to ferrite = 9373 cal per mole[4].

y_γ = Mole fraction of X in austenite.

x_γ = Mole fraction of carbon in austenite.

The temperature at which austenite and ferrite of the same composition are in metastable equilibrium is commonly termed as T_o. It is obtained by employing the condition $\Delta F^{\gamma\to\alpha} = 0$ and solving for x_γ as a function of temperature by trial and error.

So far it has been possible to evaluate $\Delta F^{\gamma\to\alpha}$ and To for pure iron, Fe-X and Fe-X-C alloys using the original concept of Zener. However, there are other alternate approachs based on the standard chemical thermodynamic expression for evaluation of $\Delta F^{\gamma\to\alpha}$ and T_o These models differ from each other in the way the emperical relationship for a_γ and a_{Fe_γ} are substituted in the following expression:

$$\Delta F^{\gamma\to\alpha} = RT\ \left[\ x_\gamma\ \ln\ \frac{a^{\gamma\alpha}_\gamma}{a_\gamma} + (1-x_\gamma)\ \ln\ \frac{a^{\gamma\alpha}_{Fe_\gamma}}{a_{Fe_\gamma}}\ \right] \quad .. \quad .. \quad .. \quad .. \quad .. \quad (A2.5)$$

Bhadeshia et al[5, 6] recently developed an expression to evaluate 'T_o'. He assumed that the carbon content of ferrite equals that of the austenite at T_o. He also consider the Zener ordering[7] while developing expresssion for 'T_o'. These assumptions yield :

$$\Delta F^{\gamma\to\alpha} = 2xRT \ln x + x(\Delta\bar{H}_\alpha - \Delta\bar{H}_\gamma - (\Delta S_\alpha - \Delta S_\gamma)T + 4w_\alpha - 6w_\gamma)$$

$$- 4RT(1 - x)\ln(1 - x) + 5RT(1 - 2x)\ln(1 - 2x)$$

$$- 6RTx \ln \frac{\delta_\gamma - 1 + 3x}{\delta_\gamma + 1 - 3x} - 6RT(1 - x)\ln \frac{1 - 2\tau_\gamma + (4\tau_\gamma - 1)x - \delta}{2\tau_\gamma(2x - 1)}$$

$$+ 3RTx \ln(3 - 4x) + 4RTx \ln \frac{\delta_\alpha - 3 + 5x}{\delta_\alpha + 3 - 5x}$$

$$+ (1 - x)\left[141\sum_i Yi\Delta T_{Mag} - \Delta T_{NM}) + \Delta F^{\gamma\to\alpha}\left(T - 100\sum_i Yi\Delta T_{Mag}\right)\right] \div \Delta f^* \quad .. \quad (A2.6)$$

where $\delta_\alpha = \left[9 - 6x(2\tau_\alpha + 3) + (9 + 16\tau_\alpha)x^2\right]^{\frac{1}{2}}$

$\delta_\gamma = \left[1 - 2(1 + 2\tau_\alpha)x + (1 + 8\tau_\gamma)x^2\right]^{\frac{1}{2}}$

$\tau_\alpha = 1 - \exp(-w_\alpha/RT)$

$\tau_\gamma = 1 - \exp(-w_\gamma/RT)$

$\Delta\bar{H}_\alpha = 112212 \text{ J mole}^{-1}$

$\Delta S_\alpha = 51.5 \text{ J mole}^{-1} \text{ K}^{-1}$

$\Delta\bar{H}_\gamma = 38575 \text{ J mole}^{-1}$

$\Delta S_\gamma = 13.48 \text{ J mole}^{-1} \text{ K}^{-1}$

Based on this method, T_o temperature has been calculated for the Fe-C-X alloy used for study of growth kinetics of ferrite. The T_o - x curve is ploted for each alloy and represented in Fig A.2.1. In solving the equation (A2.6), Δf^* = Energy term due to Zener order is evaluated as in Ref[7], w_γ is calculated using ref[8, 9], w_α from ref[10, 11]. The value of $\Delta\bar{H}_\alpha$, ΔS_α, $\Delta\bar{H}_\gamma$ and ΔS_γ are obtained from ref 11 and ref 8 respectively.

Similarly the equation for Ae'_3 (transformation without partioning) is given[8] by

$$141\sum_i Yi(\Delta T_{Mag} - \Delta T_{NM}) + \Delta F^{\gamma\rightarrow\alpha}\left(T - 100\sum_i Yi\Delta T_{Mag}\right)$$

$$= 5RT\ln\left(\frac{1-x}{1-2x}\right) + 6RT\left[\ln\frac{1-2\tau_\gamma+(4\tau_\gamma-1)x - \sqrt{1-2(1+2\tau_\gamma)x+(1+8\tau_\gamma)x^2}}{2\tau_\gamma(2x-1)}\right] \quad \text{(A2.7)}$$

In evaluating equations (A2.6) and (A2.7), the values of $\Delta F^{\gamma\rightarrow\alpha}$ are obtained from ref 17. Both T_o and Ae'_3 are plotted vrs x and represented in Fig. A2.1.

Various nomenclature used in above equations are listed in table A2.1

TABLE A2.1

Nomenclature

a_{γ} = Activity of carbon in austenite

$a_{\gamma}^{\gamma\alpha}$ = Activity of carbon at $\gamma/(\alpha+\gamma)$ phase boundary.

$a_{Fe_{\gamma}}$ = Activity of iron in austenite.

$a_{Fe_{\gamma}}^{\gamma\alpha}$ = Activity of iron at $\gamma/(\alpha+\gamma)$ phase-boundary.

R = Gas constant.

T = Absolute Temperature.

$\Delta\bar{H}_{\alpha,\gamma}$ = Partial molar heat of solution of carbon in austenite.

$\Delta S\alpha,\gamma$ = Partial molar non-configurational entropy of solution in ferrite, austenite.

$w_{\alpha,\gamma}$ = Pairwise interaction energy between adjacent carbon atoms in ferrite, austenite.

Y_i = Mole fraction of substitutional alloying element in austenite or ferrite, disregarding the presence of carbon.

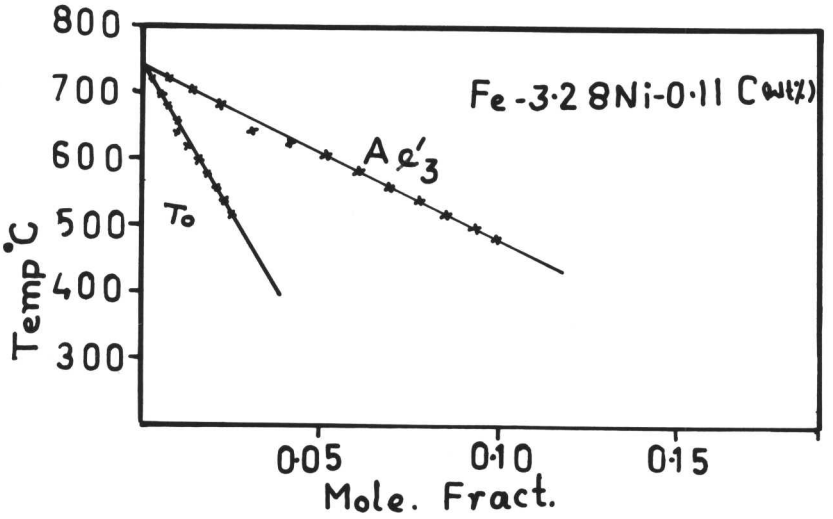

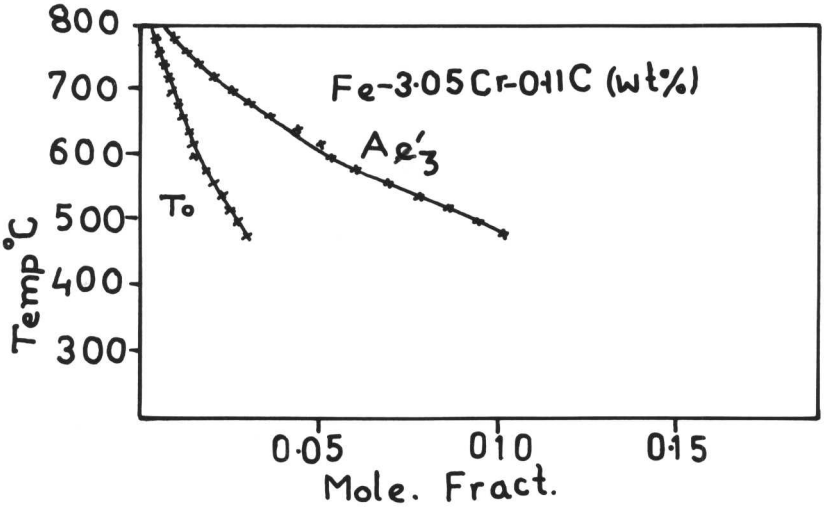

Figure A2.1: Plot of temperature vs carbon content in austenite.
(a) Fe-3.05Cr-0.11C (wt%).
(b) Fig-3.28Ni-0.11 (wt%).

APPENDIX III

NUCLEUS COMPOSITION

Study of the diffusion transformation requires a knowledge of nucleus composition. It is generally accepted that the composition of the nucleus can often be determined with the help of free energy vs composition diagram which may not necessarily represent the true composition of the nucleus during its early stage of development[1]. Gerlach[2] while working on Au-Ni alloy has found the precipitate containing higher Au-content at the beginning of precipitation than later. In order to explain why the nucleus will form with higher composition than the equilibrium, it is necessary to use the free energy diagram (Fig. A.3.1). Figure A.3.1 shows Gibbs free energy per mole for two phases (ferrite and austenite) in a Fe-C binary system. Suppose $\bar{x}$ represents the composition (i.e. carbon content) of the austenite phase (γ). Its free energy per mole is represented by the point O. The tangent at O gives the values of chemical potentials μ°_{Fe} and μ°_{C} for this composition. The chemical potential is defined by $\mu_{Fe} = dF/dn_{Fe}$ where F represents the Gibbs free energy of the specimen and n_{Fe} is the number moles Fe. Absolute chemical activity a_{Fe} can be obtained by the definition $\mu_{Fe} = RT \ln a_{Fe}$ .. ..(A3.1)

The free energy of the system can be decreased up to the point P provided it breaks up into one part of composition $x_{\gamma}^{\gamma\alpha}$ and another part of composition $x_{\alpha}^{\alpha\gamma}$. Thermodynamically the latter situation is more demanding and the nucleation of α is expected to occur with equilibrium composition $x_{\alpha}^{\alpha\gamma}$. Unfortunately formation of nucleus with equilibrium composition $x_{\alpha}^{\alpha\gamma}$ is highly unlikely[3] in presence of the surface tension as well as the strain energy involved in the nucleation of α. An additional change in free energy is required to counteract the effect arising from above two factors. This additional change in free energy can be achieved if the nucleus form with composition x_m. It is quite apparent from the Fig. A3.1 that $\Delta Fm > \Delta F$. This thermodynamically most favourable composition of the nucleus can be obtained by drawing a tangent to the curve α parallel with the tangent through the point O, representing the parent phase. The change in chemical potential referring to the nucleus composition x_m can be expressed as

$$\mu^{\circ}_{Fe} - \mu^{m}_{Fe} = \mu^{\circ}_{C} - \mu^{m}_{C} \quad .. \quad .. \quad .. \quad .. \quad .. \quad .. \quad .. \quad .. \quad .. \quad .. \quad \text{(A3.2)}$$

$$\frac{a^{\circ}_{Fe}}{a^{m}_{Fe}} = \frac{a^{\circ}_{C}}{a^{m}_{C}} \quad .. \quad .. \quad .. \quad .. \quad .. \quad .. \quad .. \quad .. \quad .. \quad .. \quad .. \quad \text{(A3.3)}$$

It is now justified that the favourable composition (C_m) for nucleation of α involves a larger change in composition (i.e. C) from the parent phase (γ) than the equilibrium value $x^{\alpha\gamma}_{\alpha}$. It is also clear from the construction of parallel tangent that with increasing supersaturation, the nucleus composition will be, pushed further away from $x^{\alpha\gamma}_{\alpha}$. Once it has been established that the composition of the nucleus x_m is thermodynamically more favourable, it is a matter of simple calculation to determine its numerical value. The numerical value of C_m can be obtained[4] by the use of following equation:

$$\Delta F^{\gamma\to\alpha}_{Fe} + RT \ln \frac{a^{\alpha}_{Fe}\,(1 - x)}{a^{\gamma}_{Fe}\,(1 - \bar{x})} - RT \ln \frac{a^{\alpha}_{C}\,(x)}{a^{\gamma}_{C}\,(\bar{x})} = 0 \quad .. \quad .. \quad .. \quad .. \quad .. \quad \text{(A3.4)}$$

$$\Delta F_m = RT \ln \frac{a^{\alpha}_{C}\,(x_m)}{a^{\gamma}_{C}\,(\bar{x})} \quad .. \quad .. \quad .. \quad .. \quad .. \quad .. \quad .. \quad .. \quad .. \quad .. \quad \text{(A3.5)}$$

For alloy steel, the first term of equation (A3.4), is replaced by[7]

$$\Delta F^{\gamma\to\alpha}_{Fe}\left\{T - 100\sum_i Y_i \Delta T_{magi}\right\} + 141\sum_i Y_i\,(\Delta T_{magi} - \Delta T_{nmi})$$

where a^{α}_{Fe} (1 - C) refers to the activity of iron in ferrite evaluated at the concentration (1 - C), and other activity terms are defined in the same way. $\Delta F^{\gamma\to\alpha}_{Fe}$ is the change in free energy accompanying the austenite-ferrite transformation of pure iron and R is the gass constant. $\bar{x}$ refers to average carbon concentration of steel and x_m represents the composition of ferrite which satisfies equation (A3.4). Y_i refers to mole fraction of ith substitutional alloying element, disregarding the presence of carbon and ΔT_{magi} and ΔT_{nmi} shift is the temperature for pure iron due to magnetic and non-magnetic components of $\Delta F^{\gamma\to\alpha}_{Fe}$ respectively. This equation can be solved iteratively or with the use of Newton-Raphson method to obtain the value of x_m in equation (A3.5), we get ΔF_m. The results of such a calculation for different alloy steels are shown in Fig. A.3.2. Experimental evidence in support of such a calculation is extremely difficult to obtain, as the critical size of the nucleus hardly exceeds the limit (= 20A°) required for resolving under TEM[5].

The most favourable composition x_m not only provides the additional driving force to counteract the effect of surface tension and strain energy but it also helps the nucleus to grow beyond the size of critical nucleus. Figure A.3.1 shows that in the equilibrium state $\mu_{Fe}^{k.1}$ has lower potential than the original specimen μ_{Fe} for Fe but for carbon, it has higher chemical potential $\mu_C^{k.1}$ than the original specimen μ_C. So it is extremely difficult for α to receive even the negligible amount of carbon during its growth for survival under equilibrium conditions. But if the nucleus forms with composition x_m, it can easily grow by receiving both kinds of atoms (i.e. Fe and C) since its chemical potential for both the components are lower than the parent phase (γ). Gradually the carbon content of the austenite becomes appreciable and pushed toward equilibrium value $x_\alpha^{\alpha\gamma}$. This gradual change in carbon content takes place in such a way that all the time both potentials are lower in α than austenite (γ).

Under special circumstances, the nuclei with a different composition may form if kinetic parameters militate in their favour. In ternary Fe-C-X system, nuclei may form with or without partitioning of a sluggish diffusing species X.[6,7] At large supersaturations, the possibility exists that unpartitioned nuclei may form, because of greater time required for alloying element redistribution. Moreover, since the no-partition nuclei have a higher free energy than the true critical nucleus, it may pass over the barrier at much greater rate and dominate the nucleation process.[5]

From the above discussion it is clear that the precipitation of alloy carbide is more favourable than the precipitation of Fe_3C since the former involves relatively large charge in free energy.[9,10] So thermodynamically precipitation of alloy carbide by interphase precipitation is more likely to occur than the cementite.

The theoretical work by Cahn and Hilliard[8] showed that the nucleus composition need not be uniform throughout. The composition fluctuation within the nucleus may be represented by

$$2K\nabla^2 C + \left(\frac{dK}{dC}\right)(\nabla C)^2 = \frac{d\Delta F}{dC}$$

where $K(\nabla C)^2$ = Gradient energy coefficient.

ΔF = Change in free energy accompanying the formation of critical nucleus.

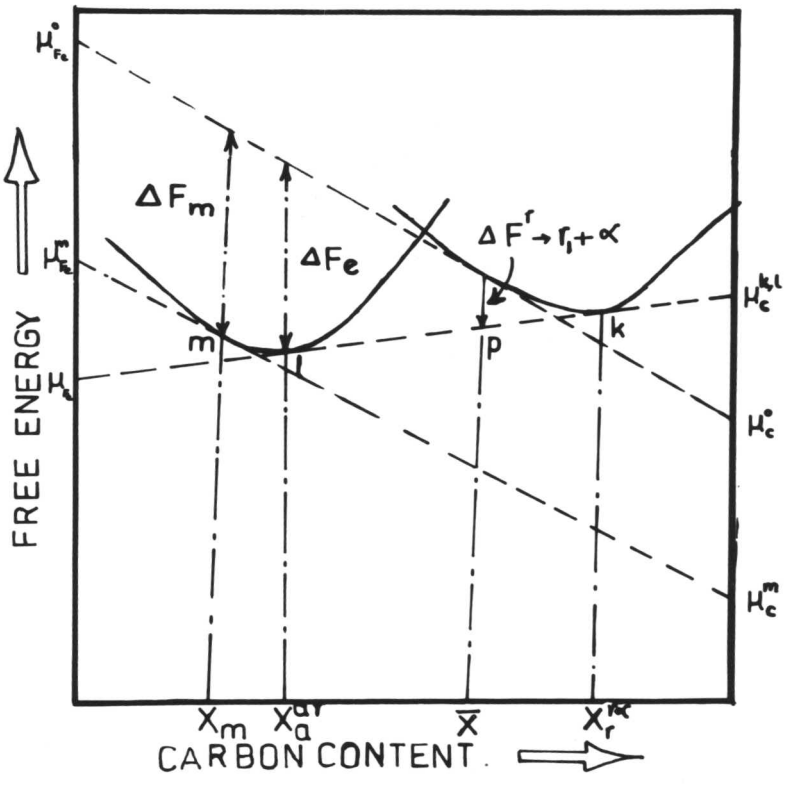
FREE ENERGY
CARBON CONTENT
ΔFm
ΔFe
m
p
k

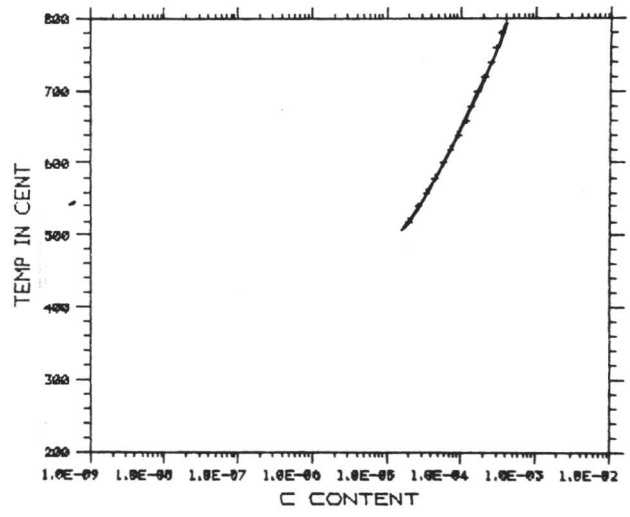

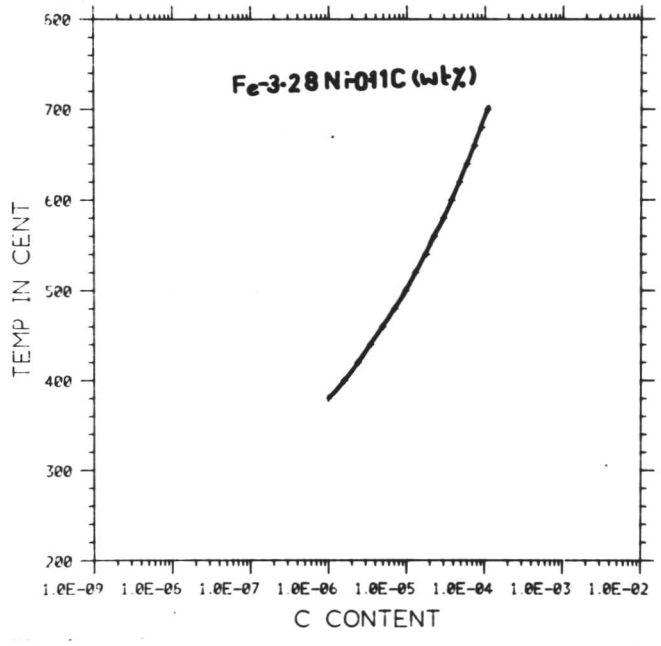

Figure A3.2: Carbon content of the nucleus vs temperature.
(a) Fe-3.05Cr-0.11C (wt%).
(b) Fe-3.28Ni-0.11C (wt%).

REFERENCES

CHAPTER II

1. Dubé, C. A., Ph.D. thesis, Carnegie Inst. of Technology, 1948.

2. Dubé, C. A., Aaronson, H. I. and Mehl, R. F., Rev. Met., 55, 201, 1958.

3. Aaronson, H. I., Decomposition of Austenite by Diffusional Processes, p. 387 ff: Interscience Publishers, New York, 1962.

4. Toney, S. and Aaronson, H. I., Trans. AIME, 221, p. 909, 1961.

5. Aaronson, H. I., Triplett, W. B. and Andes, G. M., Trans. AIME, 218, 331, 1960.

6. Hawbolt, B. and Brown, L. C., Trans. AIME, 239, p. 1916, 1967.

7. Clark, J. B., High Temperature, High-Resolution Metallography, p. 347, Gordon and Breach, New York, 1967.

8. Aaron, H. B. and Aaronson, H. I., Symposium on Altering the Time Cycle of Heat Treatment, Met. Soc. AIME, 1969.

9. Kelly, A. and Nicholson, R. B., Precipitation Hardening, Progress in Materials Science, 10, No. 3, 1963.

10. Townsend, R. D. and Kirkaldy, J. S., Trans. A.S.M., 61, p. 605, 1968,

11. Kurdjumov, G. and Sachs, G., Z. Physik, 64, p. 325, 1930.

12. Aaronson, H. I., Symposium on the Mechanism of Phase Transformations in Metals, Institute of Metals, London, p. 47, 1955.

13. Mehl, R. F., Barrett, C. S. and Smith, D. W., Trans. AIME, Vol. 105, p. 215, 1955.

14. Nabarro, F. R. N., Proc. Phys. Soc. (London), 52, 90 (1940).

15. Nabarro, F. R. N., Proc. Roy. Soc. (London), 175, 519 (1940).

16. Molt, N. F. and Nabarro, F. R. N., Proc. Phys. Soc. (London), 52, 86, 1940.

17. Smith, C. S., Trans. A.S.M., 45, 533, 1953.

18. Liu, Y. C., Aaronson, H. I., Kinsman, K. R. and Hall, M. G., Met. Trans., Vol. 3, p. 1319, 1972.

19. Hillert, M., Decomposition of Austenite by Diffusional Processes, p. 197, ff: Interscience Publishers, New York, 1962.

20. Morrison, W. B., J.I.S.I., 317, 1963.

21. Leslie, W. C. , National Physical Laboratory Symposium No. 15, "The Relationship between the Structure and Mechanical Properties of Metals", p. 333., 1963.

22. Mannerkoski, M., Acta Polytech. Scand., Ch. 26, p. 7, 1964.

23. Relander, K., Acta Polytech. Scand., Ch. 34, p. 7, 1964.

24. Tonino, M., Nishida, T., Ooka, T. and Yoshikawa, K., Proceedings of the Symposium on Micrometallurgy, Jamshedpur. 1965

25. Suzuki, H. G. and Tonino, M., Trans. I.S.I.J., 12, 217, 1972.

26. Suzuki, H,. G. and Tonino, M., Trans. I.S.I.J., 13, 80, 1973.

27. Gray, J. M. and Yeo, R. B. G., Trans. A.S.M., 61 , 255, 1968.

28. Davenport, A. T. D., Berry, F. G. and Honeycombe, R. W. K., Met. Sci. J., 2, 104, 104, 1968.

29. Baker, R. G. and Nutting, J., I.S.I., Sp. Report No. 64, 1, 1959.

30. Freeman, S., I.S.I., Report No. 45, 152, 1971.

31. Berry, F. G. and Honeycombe, R. W. K., Met. Trans. Trans., 1, 3279, 1970.

32. Davenport, A. T. D. and Honeycombe, R. W. K., Proc. Royal Soc., London, A322, 191}. 1971.

33. Campbell, K., Ph.D. Thesis, March 1971.

34. Ricks, R. A., Howell, P. R. and Honeycombe, R. W. K., Met. Trans., 10A p. 1049, 1979.

35. Ricks, R. A., J. Mat. Sci., J. Mat. Sci., 16, p. 3006, 1981.

36. Campbell, K. and Honeycombe, R. W. K., Met. Sci., 8, 197, 1974.

37. Mannerkoski, M., Met. Sci. J., 3, 54, 1969.

38. Heikkinen, V. K., Acta Met., 21, 709, 1973.

39. Heikkinen, V. K., Scand. J. Met., 109, 112, 1973a.

40. Ricks, R. A. and Howell, P. R., Metal Science, 317, June 1982.

41. Ricks, R. A. and Howell, P. R., Acta Met., Vol. 31, No. 6, p. 853, 1983.

CHAPTER III

References

1. Davenport, A.T.: M. Tech. Thesis; University of Sheffield, May 1964.

2. Hilliard, J.E., and Cahn, J.W.: Trans. AIME 1961, 221, 244.

3. Yand, J.R. and Bhadeshia, H.K.D.H.: Unpublished work; University of Cambridge.

CHAPTER IV

References

1. Honeycombe, R.W.K., Met. Trans., p. 915, July 1976.

2. Aaronson, H.I., Plichta, M.R., Franti, G.W., Russell, K.C., Met. Trans. A., Vol. 9A, p. 363, 1970.

3. Ricks, R.A. and Howell, P.R., J. of Metal Sci., 18, 3393, 1983.

4. Ricks, R.A. and Howell, P.R., Metal Sci., Vol. 16, 317, 1982.

5. Ricks, R.A. and Howell, P.R., Acta Met., Vol. 31, No. 6, p. 853, 1983.

6. Kuo, K., J.I.S.I., April 1953.

7. Lupton, J.B. et al, Met. Trans., Vol. 3, 2923, 1972.

8. Davenport, A.T. and Honeycombe, R.W.K., Proc. Roy. Soc., Lond., A322, 191, 1971.

9. Bjorn Uhrenius, Hardenability Concepts with Applications to Steels, Edts. D.V. Doane and J.S. Kirkaldy, p. 20, Feb. 1978.

10. Goldschmidth, H.J., Interstitial Alloys, Butterworth and Co. (Publishers) Ltd., 1967.

11. Wilyman, P.R. and Honeycombe, R.W.K., Metal Sci., Vol. 16, p. 295, June 1982.

12. Kinsman, K.R., Eichen, E. and Aaronson, H.I., Met. Trans., Vol. 6A, Feb. 303, 2975.

13. Jones, G.J. and Trivedi, R., J. App. Phys., 42, 4299, 1971.

14. Jones, G.J. and Trivedi, R., J. Cryst. Growth, 29, 155, 1971.

15. Bhadeshia, H.K.D.H., Phys. State Solid (a), 69, 745, 1982.

16. Cahn, R.W. and Hassen, P., Physical Metallurgy, 3rd edition, 1983.

17. Johnson, W.C. et al, Met-Trans. A, 6A, 911, 1975.

18. Cahn, R.W., Acta Met., 4, 449, 1956.

19. Smith, C.S., Trans. A.S.M., Vol. 45, p. 533, 1953.

20. Howell, P.R. and Honeycombe, R.W.K., Proceedings of an Int. Conf. on Solid-Solid Phase Transformations, edited by Aaronson, H.I. et al, Aug. 1981, p. 399.

21. Ryder, P.L., Pitch, W. and Mehl, R.F., Acta Met. 15, 1431, 1967.

22. King, A.D. and Bell, T., Met. Sci. J., 8, 253, 1974.

23. King, A.D. and Bell, T., Met. Trans. A, 6A, 1419, 1975.

24. King, A.D. and Bell, T., Metall., 9, 397, 1976.

25. Aaronson, H.I., Decomposition of Austenite by Diffusional Processes, p387, ff, Interscience Publishers, New York, 1962.

REFERENCES

CHAPTER V

1. Kinsman, K.R. and Aaronson, H.I., "Transformation and Hardenability in Steels", Climax Molybdenum Co., Ann Arbor, Mich., p.39, 1967.

2. Hillert, M., Jernkontorets Ann., 141, 757, 1957.

3. K.R. Kinsman and H.I. Aaronson. Metall. Trans., Vol. 4, P.959, 1973.

4. C. Atkinson, H.B. Aaron, K.R. Kinsman and H.I. Aaronson, Metall. Trans., Vol. 4, P.783, 1973a.

5. Aaronson, H.I., Laird, C. and Kinsman, K.K., Phase Transformation, A.S.M., Metals Park, Ohio, 1970.

6. Honeycombe, R.W.K., Met. Trans., Vol. 7A, 915, 1976.

7. Berry, F.G. and Honeycombe R.W.K., Met. Trans., 1, 3279, 1970.

8. Balliger, N.K. and Honeycombe, R.W.K., Met. Trans., 11A, 421, 1980.

9. Sakuma, T. and Honeycombe, R.W.K. Unpublished work.

10. Kuo, K., J.I.S.I., p. 363, April 1953.

11. Lupton, J.B., Murphy, S. and Wookhead, J.H., Met. Trans., Vol. 3, 2923, 1972.

12. Davenport, A.T. and Honeycombe, R.W.K., Proc. Roy. Soc., Lond., A, 322, 191 - 205, 1971.

13. Goldschmidt, H.J., Interstitial Alloys, Butterworth and Co. (Publishers) Ltd., 1967.

14. Storms, E.K. "The refactory carbides". P6; 1967. Academic Press, New York.

15. Pickering, F.B. and Gladman, T. ISI Spec. Rep. 81, P10, 1963.

16. Smith, C.S., Trans. A.S.M., Vol. 45, P533, 1953.

17. Hillèrt, M., "The Decomposition of Austenite by Diffusional Processes", Interscience, New York, P197, 1962.

18. Ryder, P.L., Pitsch, W. and Mehl, R.F., Acta Met., 15, 1431, 1967.

19. King, A.D. and Bell, T., Met. Sci. J., 8, 253, 1974.

20. King, A.D. and Bell, T., Met. Trans. A, 6A, 1419, 1975.

21. Howell, P.R. and Honeycombe, R.W.K., "Solid-Solid Phase Transformation", edited by Aaronson, P399, 1983.

22. Aaronson, H.I., "Decomposition of Austenite by Diffusional Processes", P387 ff, Interscience Publishers, New York, 1962.

23. Aaronson, H.I., Plichta, M.R., Franti, G.W. and Russell, K.C., Met. Trans., 9A, 363, 1978.

24. Coates, D.E., Met. Trans., Vol. 4, 2313, October 1973.

25. Teizchi, A. and George, K., Met. Trans. A., Vol. 14A, 261, 1983.

26. Gilmour, J.B., Purdy, G.R. and Kirkaldy, J.S., Met. Trans., Vol. 3, P3213, 1972.

27. Aaronson, H.I. and Domain, H.A., Trans. TMS-AIME, Vol. 236, P761, 1966.

CHAPTER VI

References

1. Honeycombe, R.W.K.: Effect of Second Phase Particles on the Mechanical Properties of Steel, ISI, p. 136, 1971.
2. Batte, A.D. and Honeycombe, R.W.K.: JISI, Vol. 221, p. 187, 1973.
3. Irvine, K.J.: 'Strong, Tough Structural Steels', Special Publ., Vol. 104, p. 1, 1967, London (Iron Steel Inst.).
4. Honeycombe, R.W.K.: Met. Trans., Vol. 7A, No. 7, p. 915, 1976.
5. Batte, A.D. and Honeycombe, R.W.K.: JISI, Vol. 211, p. 284, 1973.
6. Berry, F.G. and Honeycombe, R.W.K.: Met. Trans., Vol. 1, p. 3279, 1970.
7. Berry, F.G.: Ph.D. Dissertation, University of Sheffield, 1968.
8. Davenport, A.: Ph.D. Dissertation, University of Sheffield, 1968.
9. Ohmori, Y.: Ph.D. Dissertation, University of Cambridge, 1969.
10. Freeman, S.: Ph.D. Dissertation, University of Cambridge, 1971.
11. Campbell, K.: Ph.D. Dissertation, University of Cambridge, 1971.
12. Law, N.C.: Ph.D. Dissertation, University of Cambridge, 1977.
13. Balliger, N.K.: Ph.D. Dissertation, University of Cambridge, 1977.
14. Southwick, P.D.: Ph.D. Dissertation, University of Cambridge, 1978.
15. Ricks, R.A.: Ph.D. Dissertation, University of Cambride, 1979.
16. Parsons, S.A.: Ph.D. Dissertation, University of Cambridge, 1981.
17. Howell, P.R. and Honeycombe, R.W.K.: Int. Conf. on Solid-Solid-Phase Transformations, ed. H.I. Aaronson et al., AIME publications, p. 399. 1982.
18. Predel, B. and Gust, W.: Mat. Sci., Engg., Vol. 17, p. 41, 1975.
19. Liu, Y.C. and Aaronson, H.I.: Acta Met. Vol. 16, p. 1343, 1968.
20. Gust, W., Predel, B. and Nguyen, Tal L.: Z. Metallkde, Vol. 67, p. 110, 1976.
21. Tu, K.N. and Turnbull, D.: Acta Met., Vol. 15, p. 369, 1967.
22. Fournelle, R.A. and Clark, J.B.: Met. Trans., Vol. 3, p. 2757, 1972.
23. Fournelle, R.A.: Acta Met. p. 1135, 1979.
24. Geisler, A.H.: Phase Transformations in Solids, p. 387, Wiley, 1951.
25. Rosenbaum, H.S. and Turnbull, D.: Acta Met., Vol. 7, p. 664, 1959.
26. Thomas, G. and Nutting, J.: Inst. of Metals, Vol. 88, p. 81, 1959-60.

CHAPTER VII

References

1. Morrison, W.B.: J. Iron Steel Inst., London 201, 317 (1963).

2. Fisher, G.L. and Geils, R.H.: Trans. Metall. Soc. AIME 245, 2405 (1969).

3. Serin, B., Desalas, Y., Maitrepierre, Ph. and Rofes-Vernis, J.: Mem. Sci. Rev. Metall., 75, 355 (1978).

4. Thomas, M.H. and Michal, G.M.: Proce. of Int. Conf. on Solid-Solid Phase Transformations; edited by H.I. Aaronson, D.E. Laughlin, R.F. Sekeyka and C.M. Wayman, Aug. 10-14, 1981, JMS-AIME, Warrendale, Pennsylvania, p. 399, 1981.

5. Maitrepierre, Ph., Thivellier, D., Rofes-Vernis, J., Rosseare, D. and Tricot, R.: Hardenability concepts with applications to steel. The Metallurgical Society of AIME, 421 (1978).

6. Ohmori, Y.: Trans. Iron Steel Inst., Japan 11, 339 (1971).

CHAPTER VIII

References

1. Ham, F.S.: Jnl. App. Phy. 20, p. 950. 1959.

2. Aaronson, H.I.: Phase-Transformations, York Conference, Insitute of Metallurgists, London, p. 11-1, 1979.

3. Coates, D.E.: Met. Trans., Vol. 4, p. 2313, 1973.

4. Coates, D.E.: Met. Trans., Vol. 3, p. 1203, 1972.

5 . Trivedi, R. and Pound, G.M.: J. Appl. Phys., Vol. 38, p. 3569, 1967.

6. Brown, L.C.: J. Appl. Phys., Vol. 43, p. 4443, 1972.

7. Bolze, G., Coates, D.E. and Kirkaldy, J.S.: Met. Trans., Vol. 62, p. 959, 1969.

8. Hillert, M.: Internal Report, Swedish Institute of Metals Research, 1953.

9. Kirkaldy, J.S.: Canda. J. Physics, 36, 907, 1958.

10. Purdy, G.R., Weichert, D.H. and Kirkaldy, J.S.: Trans. TMS-AIME, Vol. 230, p. 1025, 1964.

11. Hultgren, A.: Trans. ASM, Vol. 39, p. 915, 1947.

12. Hillert, M.: Jernkont. Ann; Vol. 136, p. 25, 1952.

13. Rudberg, E.: Jernkont. Ann; Vol. 136, p. 91, 1952.

14. Aaronson, H.I., Domain, H.A. and Pound, G.M.: Trans. TMS-AIME; Vol. 236, p. 768, 1966.

15. Gilmour, J.B., Purdy, G.R. and Kirkaldy, J.S.: Met. Trans., Vol. 3, p. 1455, 1972.

16. Bhadeshia, H.K.D.H.: Diffusional Formation of Ferrite in Iron and its Alloys, Prog. Mat. Sci., Vol. 29, pp. 328-386, 1985.

17. Wagner, C.: Thermodynamics of Alloys, p. 51, Addison-Wesley, Reading, Mass., 1952.

18. Purdy, G.R. and Kirkaldy, J.S.: TMS-AIME, Vol. 227, p. 1255.

19. Purdy, G.R., Weichert, D.H. and Kirkaldy, J.S.: TMS-AIME, Vol. 230, p. 1025, 1964.

20. Kinsman, K.R. and Aaronson, H.I.: 'Transformation and Hardenability in Steels', Climax Moly. Co., Ann Arbor, Mich., p. 39, 1969.

21. Kinsman, K.R. and Aaronson, H.I.: Metall. Trans., Vol. 4, p. 959, 1973.

22. Bradley, J.R. and Aaronson, H.I.: Metall. Trans. A., Vol. 8A, p. 317, 1977.

23. Bradley, J.R. and Aaronson, H.I.: Metall. Trans. A., Vol. 12A, p. 1729, 1981.

24. Hillert, M.: The Mechanism of Phase-Transformation in Crystalline Solids, edited by Inst. of Metals, London, p. 231, 1969.

25. Aaronson, H.I. and Domain, H.A.: TMS-AIME, Vol. 236, p. 781, 1966.

26. Zener, C.: J. Appl. Phys., Vol. 20, p. 950, 1949.

27. Christian, J.W.: Theory of Phase-Transformation in Metals and Alloys, 2nd edition, Part I, p. 482, Pergamon Press, Oxford, 1975.

28. Bhadeshia, H.K.D.H.: Metal-Science, 15, p. 175, 1981.

29. Bhadeshia, H.K.D.H.: Metal-Science, 15, p. 178, 1981.

30. Bhadeshia, H.K.D.H. and Edmonds, D.V.: Acta-Metall., Vol. 28, p. 1265, 1980.

31. Bhadeshia, H.K.D.H.: Metal-Science, Vol. 15, p. 477, 1981.

32. Bhadeshia, H.K.D.H.: Unpublished work, University of Cambridge.

33. Kinsman, K.R. and Aaronson, H.I.: Transformation and Hardenability in Steels, p. 39, Climax Molybdenum Co., Ann Arbor, Michigan, 1967.

34. Kinsman, K.R. and Aaronson, H.I.: Metall. Trans., Vol. 4, p. 959, 1973.

35. Atkinson, C., Aaron, H.B., Kinsman, K.R. and Aaronson, H.I.: Met. Trans., Vol. 4, p. 783, 1973.

36. Bradley, J.R., Rigsbee, J.M. and Aaronson, H.I.: Metall. Trans. A, Vol. 8A, p. 323, 1977.

37. Hillert, M.: Decomposition of Austenite by Diffusional Processes, eds. Zackay and Aaronson, p. 387, Interscience, 1962.

38. Ryder, P.L., Pitsch, W. and Mehl, R.F.: Acta Met., Vol. 15, p. 1431, 1967.

39. King, A.D. and Bell, T.: Met. Sci. J., Vol. 8, p. 253, 1974.

40. King, A.D. and Bell, T.: Met. Trans. A, Vol. 6A, p. 1419.

41. Aaronson, H.I.: Decomposition of Austenite by Diffusional Processes, p. 287, Interscience, eds. Zackay and Aaronson, 1962.

42. Aaronson, H.I., Laird, C. and Kinsman, K.R.: Phase Transformations, p. 313, ASM, Metal Park, Ohio, 1970.

43. Honeycombe, R.W.K.: Met. Trans. A, Vol. 7A, p. 915, 1976.

44. Honeycombe, R.W.K.: Met. Trans. A, Vol. 7A, p. 915, 1976.

45. Purdy, G.R.: Acta Metall., Vol. 26, p. 477, 1978.

46. Middleton, C.J. and Edmonds, D.V.: Metallography, Vol. 10, p. 55, 1977.

47. Bradley, J.R. and Aaronson, H.I.: Met. Trans., A, Vol. 12A, p. 1729, Oct. 1981.

48. Uhrenius, B.: Hardenability Concepts with Applications to Steels, eds. D.D. Doane and J.S. Kirkaldy, AIME publications, p. 28, 1978.

49. Gilmour, J.B., Purdy, G.R. and Kirkaldy, J.S.: Metall. Trans., Vol. 3, p. 3213, 1972.

50. Hillert, M.: Acta Met., Vol. 3, p. 34, 1955.

51. Hillert, M.: Mech. of Phase Transformations in Cryst. Solids, Institute of Metals (London), Monograph 13, p. 231, 1969.

52. Shiflet, G.J., Aaronson, H.I. and Bradley, J.R.: Met. Trans. A, Vol. 12A, p. 1743, 1981.

53. Cahn, J.W.: Acta Met., Vol. 10, p. 789, 1962b.

54. Sharma, R.C. and Purdy, G.R.: Metall. Trans., Vol. 4, p. 2303, 1973.

55. Kirkaldy, J.S. and Baganis, E.A.: Metall. Trans. A, Vol. 9A, p. 495, 1978.

56. Boswell, P., Kinsman, K.R. and Aaronson, H.I.: Unpublished work, Ford Motor Co., Dearborn, Michigan, 1968.

57. Aaronson, H.I. and Domain, H.A.: TMS-AIME, Vol. 236, p. 768, 1966.

58. Clemm, P.J. and Fisher, J.C.: Acta Met., Vol. 3, 70, 1955.

59. Gronsky, R. and Furrer, P.: Met. Trans. A, Vol. 12A, p. 121, 1981.

60. Dubé, C.A.: Ph.D. Thesis, Carnegie Institute of Technology, 1948.

61. Howell, P.R. and Honeycombe, R.W.K.: Proc. Int. Conf. on Solid-Solid Phase Transformation: TMS-AIME, Warrendale, Pennsylvania, p. 399, 1981.

62. Cahn, J.W.: Acta Met., Vol. 8, p. 554, 1960.

63. Bhadeshia, H.K.D.H.: Acta Met., Vol. 29, p. 1117, 1981.

64. Kinsman, K.R., Eichen, E. and Aaronson, H.I., Met. Trans., Vol. 6A, p. 303, 1975.

65. Aaronson, H.I.: Decomposition of Austenite by Diffusional Processes, p. 387, ff, Interscience Publishers, New York, 1962.

66. Russell, K.C.: Phase Transformations, p. 219, ASM, Metal Park, Ohio, 1970.

67. Avrami, M.: J. Chem. Phys., Vol. 7, 1103, 1939, 1 bid: 8.212, 1940, 1 bid. 9, 177, 1941.

68. Mazanec, K. and Cadek, J., Rev. Met., Vol. 212, p. 501, 1958.

69. Christian, J.W.: 'The Theory of Phase Transformations in Metals and Alloys', Pergamon Press, London, 1965.

CHAPTER IX

References

1. Bhadeshia, H.K.D.H.: Metal Science, Vol. 16, p. 159, March 1982.

2. Christian, J.W.: 'Theory of Transformations in Metals and Alloys', 2nd edition, Pt. 1, Pergamon Press, Oxford (1975).

3. Honeycombe, R.W.K.: Carbide Precipitation in Ferrite, Proc. of an Inter. Conf. on Phase Transformation in Ferrous Alloy (1983), AIME, ed. by A.R. Marder and J.I. Goldstein.

4. Christian, J.W.: 'Theory of Transformations in Metals and Alloys', Pergamon Press, Oxford, (1965).

5. Cahn, J.W.: Acta Met., Vol. 5, p. 169, March 1957.

6. Dollins, C.C.: Acta Met., Vol. 18, p. 1209, November 1970.

7. Ashby, M.F. and Brown, L. M.: Phil. Mag., Vol. 8, p. 1083, 1963.

8. Ohmori, Y.: Ph.D. Dissertation, University of Cambridge, 1969.

9. Davenport, A.T. and Becker, P.C.: Met. Trans., Vol. 2, p. 2962, 1971.

10. Batte, A.D. and Honeycombe, R.W.K.: J. Iron and Steel Inst., Vol. 211, p. 284, 1973.

11. Law, N.C.: Ph.D. Dissertation, University of Sheffield, 1968.

12. Campbell, K. and Honeycombe, R.W.K.: Met. Sci., Vol. 8, p. 197, 1974.

13. Berry, R.G. and Honeycombe, R.W.K.: J. Iron and Steel Instit., Vol. 211, p. 284, 1973.

14. Howell, P.R. et al.: Phil. Mag., Vol. 41 (2), p. 165, 1980.

15. Davenport, A.T. and Honeycombe, R.W.K.: Proc. Roy. Soc., Vol. A332, p. 191, 1971.

16. Shiflet, G.J., Aaronson, H.I. and Bradley, J.R.: Met. Trans. A, Vol. 12A, p. 1743, 1981.

APPENDIX I

References

1. Bhadeshia, H.K.D.H.: Metal Science, Vol. 16, p. 159, March 1982.

2. Russell, K.C.: Acta Metall., Vol. 16, p. 761, 1968.

3. Russell, K.C.: Acta Metall., Vol. 17, p. 1123, 1969.

4. Kirkaldy, J.S. et al.: Hardenability concepts with applications to steels, p. 82, 1978, Metals Park, Ohio, U.S.A., ASM.

5. Hillert, M.: Acta Metall., Vol. 1, p. 764, 1953.

6. Aaronson, H.I. et al.: Trans. Met. Soc., AIME, Vol. 236, p. 768, 1966.

APPENDIX II

References

1. Zener, C.: AIME Trans., Vol. 167, p. 513, 1946.

2. Zener, C.: AIME Trans., Vol. 203, p. 619, 1955.

3. Aaronson, H.I., Domain, H.A. and Pound, G.M.: Trans. Met. Soc., AIME, vOL. 236, p. 768, 1966.

4. Aaronson, H.I., Domain, H.A. and Pound, G.M.: Trans. Met. Soc., AIME, Vol. 236, p. 753, 1966.

5. Bhadeshia, H.K.D.H. and Edmonds, D.V.: Acta Met., Vol. 28, p. 1265, 1980.

6. Bhadeshia, H.K.D.H.: Unpublished work.

7. Fisher, J.C.: Met. Trans. Vol. 185, p. 688, 1949.

8. Shiflet, G.J., Bradley, J.R. and Aaronson, H.I.: Metall. Trans. A, Vol. 9, p.999, 1978.

9. Oblak, J.M. and Hehemann, R.F.: Transformations and Hardenability in Steels, p. 15, Climax Moly, Ann Arbor, 1967.

10. Bhadeshia, H.K.D.H.: Metal Sci. J. (1980).

11. Lobo, J.A. and Geiger, G.H.: Metall. Trans. A, Vol. 7, p. 1347, 1976.

12. Kaufman, L., Clougherty, E.V. and Weiss, R.J.: Acta Metall., Vol. 11, p. 323, 1963.

APPENDIX III

References

1. Hillert, M.: Acta Metall., Vol. 1, p. 764, 1953.

2. Gerlach, W.: Z. Metalk., Vol. 40, p. 281, 1949.

3. Hillert, M.: Lectures on the Theroy of Phase Transformations, Ed. Aaronson, H.I., AIME, May 20, 1974, pp. 1-44.

4. Bhadeshia, H.K.D.H.: Metal Science, Vol. 16, p. 159, March 1982,

5. Russell, K.C.: Phase Transformations, p. 219, ASM, Metal Park, Ohio, 1969.

6. Aaronson, H.I., Domain, H.A. and Pound, G.M.: Trans. TMS-AIME, Vol. 236, p. 768, 1966.

7. Aaronson, H.I., Domain, H.A.: Trans. TMS-AIME, Vol. 236, p. 781, 1966.

8. Cahn, J.W. and Hilliard, J.E.: Journal of Chemical Physics, Vol. 31, No. 3, p. 688, 1959.

9. Entin, R.I.: Decomposition of Austenite by Diffusional Process, p. 295, Interscience Publishers, New York, 1962.

10. Colters, R.G.: Materials Science and Engineering, Vol. 76, p. 10, 1985.